Free Vibration of Bi-directional Functionally Graded Material Circular Beams using Shear Deformation Theory employing Logarithmic Function of Radius

Jamshid Fariborz

Thesis submitted to the faculty of the Virginia Polytechnic Institute and State University in partial fulfillment of the requirements for the degree of

Master of Science

In

Mechanical Engineering

Romesh C. Batra (Chair)

Pablo A. Tarazaga

Reza Mirzaeifar

August 27th 2018

Blacksburg, VA

Keywords: Free Vibration, Bi-directional Grading, Circular Beams,

Logarithmic Shear Deformation Theory

Copyright 2018, Jamshid Fariborz

Free Vibration of Bi-directional Functionally Graded Material Circular Beams using Shear Deformation Theory employing Logarithmic Function of Radius

Jamshid Fariborz

ABSTRACT

Curved beams such as arches find ubiquitous applications in civil, mechanical and aerospace engineering, e.g., stiffened floors, fuselage, railway compartments, and wind turbine blades. The analysis of free vibrations of curved structures plays a critical role in their design to avoid transient loads with dominant frequencies close to their natural frequencies. One way to increase their applications and possibly make them lighter without sacrificing strength is to comprise them of Functionally Graded Materials (FGMs) that are composites with continuously varying material properties in one or more directions.

In this thesis, we study free vibrations of FGM circular beams by using a logarithmic shear deformation theory that incorporates through-the-thickness logarithmic variation of the circumferential displacement, does not require a shear correction factor, and has a parabolic through-the-thickness distribution of the shear strain. The radial displacement of a point is assumed to depend only upon its angular position. Thus the beam theory can be regarded as a generalization of the Timoshenko beam theory. Equations governing transient deformations of the beam are derived by using Hamilton's principle. Assuming a time harmonic variation of displacements, and by utilizing a generalized differential quadrature method (GDQM), the free vibration problem is reduced to solving an algebraic eigenvalue problem whose solution provides frequencies and corresponding mode shapes. Results are presented for different spatial variations of the material properties, boundary conditions, and the beam aspect ratio. It is found that frequencies of the FGM beam are bounded by those of two geometrically identical homogeneous beams composed of the two constituents of the FGM beam. Keeping other variables fixed, the change in the beam opening angle results in very close frequencies of the first two modes of vibration, a phenomenon usually called mode transition.

Free Vibration of Bi-directional Functionally Graded Material Circular Beams using Shear Deformation Theory employing Logarithmic Function of Radius

Jamshid Fariborz

GENERAL AUDIENCE ABSTRACT

Curved and straight beams of various cross-sections are one of the simplest and most fundamental structural elements that have been extensively studied because of their ubiquitous applications in civil, mechanical, biomedical and aerospace engineering. Many attempts have been made to enhance their material properties and designs for applications in harsh environments and reduce weight. One way of accomplishing this is to combine layerwise two or more distinct materials and take advantage of their directional properties. It results in a lightweight structure having overall specific strength superior to that of its constituents. Another possibility is to have volume fractions of two or more constituents gradually vary throughout the structure for enhancing its performance under anticipated applications. Functionally graded materials (FGMs) are a class of composites whose properties gradually vary along one or more space directions. In this thesis, we have numerically studied free vibrations of FGM circular beams to enhance their application domain and possibly use them for energy harvesting.

CONTENTS

LIST OF FIGURES

LIST OF TABLES

1. Introduction

Beams are one of the simplest, most studied and indispensable elements of mechanical, civil, marine, and aeronautical structures. They are regularly used in numerous modern engineering applications. The literature is replete with studies on static and dynamic deformations of beams composed of monolithic and composite materials. Commonly studied beam theories include the Euler-Bernoulli (EB), the Timoshenko, the first order shear deformation theory (FSDT) as well as higher order shear and normal deformation theories (HSNDT) for accurately analyzing beams of various geometries.

The simplest beam theory taught in an undergraduate course is the EB theory that gives good results for slender (large length/thickness ratio) beams. It underestimates deflections and overestimates natural frequencies since it neglects transverse shear and normal deformations. The Timoshenko beam theory assumes uniform transverse shear strain through the beam thickness, and is often used to study moderately thick beams usually classified as ones with length/thickness ratio of about 10 [1]. This theory does not satisfy tangential traction boundary conditions at the top and the bottom surfaces of the beam, and generally requires a problem-dependent shear correction factor. A number of higher order shear deformation theories considering non-uniform transverse shear deformations and not requiring a shear correction factor have been proposed for studying static and dynamic deformations of beams; e.g., see [2, 3].

A majority of early works on beams considered a straight structure made of isotropic and homogeneous materials. However, modern engineering applications require more durable, lighter and thermally resistant materials than a homogeneous material. This resulted in laminated composite structures that exploit directional properties of the constituent materials [4-6]. Vel and Batra [29], amongst others, have analytically studied deformations of clamped-clamped composite laminate beams.

The discontinuity across adjoining layers of a laminated composite structure may induce premature delamination and debonding. These can be avoided by smoothly grading volume fractions of constituents and hence material properties in one or more spatial directions; such materials are called Functionally Graded Materials (FGMs) [7, 8]. The static, dynamic and buckling response of FGM

straight beams with material properties smoothly varying in the thickness direction has been extensively analyzed; e.g. see [9-14].

There have been fewer studies on FGM beams with material properties graded in both directions, and even fewer for curved beams. Qian and Batra [16] used the meshless local Petrov-Galerkin method (MLPG) to find bi-directional spatial distribution of the two constituents to optimize the fundamental frequency of a FGM beam. Goupee and Vel [17] used a genetic algorithm coupled with a numerical scheme to maximize natural frequencies of a FGM beam. Lu et al. [15] used the state-space based differential quadrature method to find a semi-analytical elasticity solution for static thermo-mechanical deformations of a bi-directional FGM beam. Free and forced vibrations of FGM Timoshenko beams under a moving load and various boundary conditions have been studied by Simsek [18]. Karamanli [19] has analyzed free vibration of bi-directional FGM straight beams using a third order shear deformation theory in which material properties vary exponentially along the beam thickness and length.

Rastgo et al. [20] have studied stability of curved FGM beams with material properties varying only in one direction and subjected to thermal loading. Shafiee et al. [30] have investigated their in-plane and out-of-plane buckling. Eroglu [21] has studied in-plane vibration of FGM circular arches by employing a FSDT. However, there are a few studies on bi-directionally graded curved beams. Recently, Pydah and Sabale [22] presented static analysis of bi-directional FGM circular beams using kinematic assumptions of the EB beam theory. Pydah and Batra [23] extended it to a quadratic distribution of the transverse shear stress through the beam thickness and simultaneously satisfy non-zero tangential tractions prescribed on beam's top and bottom surfaces. They employed a logarithmic function of the radial coordinate in the postulated expression for the circumferential displacement.

Here we use Batra and Pydah's [23] beam theory to study free vibration of homogeneous, either radially graded or bi-directionally graded circular beams of different opening angles and under various boundary conditions. For radially graded beams, material properties are assumed to vary either affinely or exponentially along the beam thickness. For a bi-directionally graded beam, we assume that a material property, Q, is given by $Q(r,\theta) = Q^* f(r) g(\theta)$ where $f(r)$ and $g(\theta)$ are, respectively, non-dimensional functions of the radial and the circumferential coordinates r and θ. We employ Hamilton's principle to derive equations of motion and boundary conditions, and a generalized differential quadrature method (GDQM) to numerically solve these equations for natural frequencies and mode shapes. The in-house developed MATLAB code, included in the Appendix, is first verified by comparing computed results

for homogeneous and radially graded FG beams with those available in the literature. Subsequently, we find natural frequencies and mode shapes for different gradation of material properties in both directions, the beam opening angle, and boundary conditions at the edges.

2. Formulation of the Problem

Figure 1 represents a schematic sketch of a circular beam of rectangular cross-section having width b, thickness h, opening angle θ_{tip}, and radius of the centroidal axis R_0.

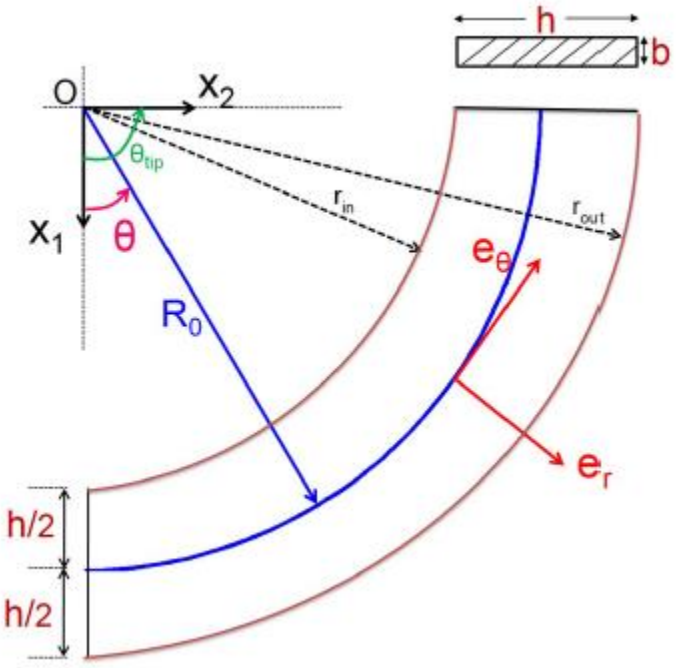

Figure 1 Geometry of a circular beam [23]

2.1. Equations of motion

We employ the recently proposed shear deformable theory [23] using a logarithmic function of the radial coordinate r to describe transverse shear deformations that satisfy tangential traction boundary conditions prescribed on beam's inner and outer surfaces. For studying plane strain free vibrations of the beam, we assume that beam's top and bottom surfaces are traction free, and boundary conditions prescribed on the edges do no work during beam's deformations. The theory assumes the following expressions for the radial and the circumferential displacements denoted, respectively, by u_r and u_θ, of a point of the beam.

$$u_r(r,\theta,t) = u_r^0(\theta,t)$$
$$u_\theta(r,\theta,t) = u_\theta^0(\theta,t) + (r-R_0)\phi(\theta,t) + U_0(r)\psi(\theta,t) \tag{2.1}$$

where

$$\psi(\theta,t) = u_\theta^0(\theta,t) - \left(u_r^0(\theta,t)\right)' - R_0\phi(\theta,t)$$
$$U_0(r) = \frac{4}{h^2}\left(r^2 - R_0^2 + r\left(1 - 2R_0 ln\left(\frac{r}{R_0}\right)\right)\right) \tag{2.2}$$

In equations (2.1) and (2.2), $u_r^0(\theta,t)$ and $u_\theta^0(\theta,t)$ are, respectively, the radial and the tangential displacements of a point on the beam centroidal axis, $\phi(\theta,t)$ represents the rotation of a cross-section about the X_3- or the z-axis (not shown in Fig.1), and $\left(u_r^0(\theta,t)\right)' = \partial u_r^0/\partial\theta$. The beam theory has three unknown fields, namely, $u_r^0(\theta,t)$, $u_\theta^0(\theta,t)$ and $\phi(\theta,t)$. It does not require a shear correction factor. For a thin beam, i.e, $h/R_0 \ll 1$, displacements (2.1) and (2.2) reduce to those for a Timoshenko beam.

We assume the beam material to be isotropic and linearly elastic (i.e., it obeys Hooke's law), and consider its infinitesimal deformations. Thus the radial, the circumferential, and the transverse shear strains, respectively, denoted by ϵ_r, ϵ_θ and $\gamma_{r\theta}$ have the following expressions.

$$\epsilon_r(r,\theta,t) = 0, \qquad \epsilon_\theta(r,\theta,t) = \frac{1}{r}\frac{\partial u_\theta}{\partial\theta} + \frac{u_r}{r}, \qquad \gamma_{r\theta}(r,\theta.t) = \frac{1}{r}\frac{\partial u_r}{\partial\theta} + \frac{\partial u_\theta}{\partial r} - \frac{u_\theta}{r} \tag{2.3}$$

By substituting for displacements from equation (2.1) into equation (2.3) we get

$$\epsilon_\theta(r,\theta,t) = \frac{1}{r}\left\{u_r^0(\theta,t) + \left(u_\theta^0(\theta,t)\right)' + (r-R_0)\left(\phi(\theta,t)\right)' + U_0(r)\left(\psi(\theta,t)\right)'\right\}$$
$$\gamma_{r\theta}(r,\theta,t) = \frac{1}{h^2 r}(h^2 - 4(r-R_0)^2)\left(\left(u_r^0(\theta,t)\right)' - u_\theta^0(\theta,t) + R_0\phi(\theta,t)\right) \tag{2.4}$$

Thus, the transverse shear strain has a quadratic variation through the beam thickness and vanishes at the top and the bottom surfaces. Recalling that $\psi(\theta,t)$ depends upon $\left(u_r^0(\theta,t)\right)'$, the expression for $\epsilon_\theta(r,\theta,t)$ has $\left(u_r^0(\theta,t)\right)''$. We introduce an auxiliary variable

$$u_1^0 = (u_r^0)' \tag{2.5}$$

and rewrite equation (2.2a) as

$$\psi(\theta,t) = u_\theta^0(\theta,t) - \left(u_1^0(\theta,t)\right) - R_0\phi(\theta,t) \tag{2.6}$$

The circumferential (or the hoop or the bending) stress σ_θ, and the transverse shear stress $\tau_{r\theta}$ are given by

$$\sigma_\theta(r,\theta,t) = \frac{E(r,\theta)}{r}\left\{u_r^0(\theta,t) + \left(u_\theta^0(\theta,t)\right)' + (r-R_0)\left(\phi(\theta,t)\right)' + U_0(r)\left(\psi(\theta,t)\right)'\right\}$$

$$\tau_{r\theta}(r,\theta,t) = G(r,\theta)\left[\frac{1}{h^2 r}(h^2 - 4(r-R_0)^2)\left(\left(u_r^0(\theta,t)\right)' - u_\theta^0(\theta,t) + R_0\phi(\theta,t)\right)\right] \tag{2.7}$$

Because of the kinematic constraint, $\epsilon_r = 0$, the radial stress is indeterminate. One can find it by using a stress-recovery scheme as was done in [23]. In equation (2.7), $E(r,\theta)$ and $\mathrm{G}(r,\theta)$ are, respectively, the shear and Young's modulii of the beam material. For a homogeneous beam, $E(r,\theta)$ and $\mathrm{G}(r,\theta)$ are constants.

The action integral, A, for the beam with kinetic energy K and potential energy U in an arbitrarily small but known time interval $[t_0, t_1]$ is defined as

$$A = \int_{t_0}^{t_1} [K - U]dt \tag{2.8}$$

We derive governing equations by using Hamilton's principle, i.e,

$$\delta A = \int_{t_0}^{t_1} [\delta K - \delta U] dt = 0 \tag{2.9}$$

where δ represents a variation. For a circular beam in the absence of external surface tractions, we have

$$\delta K = b \int_{t_0}^{t_1} \int_{R_0-\frac{h}{2}}^{R_0+\frac{h}{2}} \int_{0}^{\theta_{tip}} [\rho(r,\theta)(\dot{u}_r \delta \dot{u}_r + \dot{u}_\theta \delta \dot{u}_\theta)] r d\theta \, dr \, dt \tag{2.10a}$$

$$\delta U = b \int_{t_0}^{t_1} \int_{R_0-\frac{h}{2}}^{R_0+\frac{h}{2}} \int_{0}^{\theta_{tip}} [\sigma_\theta \delta \epsilon_\theta + \tau_{r\theta} \delta \gamma_{r\theta}] r d\theta \, dr \, dt \tag{2.10b}$$

Here ρ is mass density of the beam material, and $\dot{u}_r = \partial u_r / \partial t$.

Substitution for displacements from equations (2.1) and (2.2) into equation (2.10a) gives

$$\begin{aligned} \int_{t_0}^{t_1} \delta K dt \; = b \int_{t_0}^{t_1} \int_{0}^{\theta_{tip}} \{ & A_1 \dot{u}_r^0 \delta \dot{u}_r^0 \\ & + \left[(A_1 + I_1 + 2K_1)\dot{u}_\theta^0 + (A_2 - R_0 A_1 - 2R_0 K_1 + K_2 - R_0 I_1)\dot{\phi} - (K_1 + I_1)\dot{u}_1^0 \right] \delta \dot{u}_\theta^0 \\ & + \left[(A_2 - R_0 A_1 - 2R_0 K_1 + K_2 - R_0 I_1)\dot{u}_\theta^0 \right. \\ & \left. + (A_3 + R_0^2 A_1 + R_0^2 I_2 - 2R_0 A_2 - 2R_0 K_2 + 2R_0^2 K_1)\dot{\phi} - (K_2 - R_0 K_1 - R_0 I_1)\dot{u}_1^0 \right] \delta \dot{\phi} \\ & + \left[-(K_1 + I_1)\dot{u}_\theta^0 - (K_2 - R_0 K_1 - R_0 I_1)\dot{\phi} + I_1 \dot{u}_1^0 \right] \delta \dot{u}_1^0 \} d\theta \, dt \end{aligned} \tag{2.11}$$

where

$$A_i = \int_{R_0-\frac{h}{2}}^{R_0+\frac{h}{2}} r^i \rho(r,\theta) dr \,, \qquad K_i = \int_{R_0-\frac{h}{2}}^{R_0+\frac{h}{2}} r^i U_0 \rho(r,\theta) dr \,, \qquad I_i = \int_{R_0-\frac{h}{2}}^{R_0+\frac{h}{2}} r^i U_0^2 \rho(r,\theta) dr. \tag{2.12}$$

Similarly,

$$\int_{t_0}^{t_1} \delta U dt = b \int_{t_0}^{t_1} \int_{R_0-\frac{h}{2}}^{R_0+\frac{h}{2}} \int_{0}^{\theta_{tip}} \left[\sigma_\theta \left\{ \delta u_r^0 - U_0 \delta (u_1^0)' + (1+U_0)\delta \left(u_\theta^0\right)' + (r - R_0 - R_0 U_0)\delta \phi' \right\} \right.$$
$$\left. + \tau_{r\theta} \left(1 - \frac{4}{h^2}(r-R_0)^2\right) \left(\delta u_1^0 - \delta u_\theta^0 + R_0 \delta \phi\right) \right] d\theta \, dr \, dt \qquad (2.13)$$
$$= b \int_{t_0}^{t_1} \int_{0}^{\theta_{tip}} \left[\left\{ N \delta u_r^0 - P \delta (u_1^0)' + (N+P)\delta \left(u_\theta^0\right)' + (M - R_0 P)\delta (\phi)' \right\} \right.$$
$$\left. + \frac{1}{h^2}(h^2 F - 4R)\left(\delta u_1^0 - \delta u_\theta^0 + R_0 \delta \phi\right) \right] d\theta \, dt$$

where we have set

$$F = \int_{R_0-\frac{h}{2}}^{R_0+\frac{h}{2}} \tau_{r\theta} dr \,, \qquad R = \int_{R_0-\frac{h}{2}}^{R_0+\frac{h}{2}} (r-R_0)^2 \tau_{r\theta} dr \,, \qquad N = \int_{R_0-\frac{h}{2}}^{R_0+\frac{h}{2}} \sigma_\theta dr$$
$$M = \int_{R_0-\frac{h}{2}}^{R_0+\frac{h}{2}} (r-R_0)\sigma_\theta dr \,, \qquad P = \int_{R_0-\frac{h}{2}}^{R_0+\frac{h}{2}} U_0 \sigma_\theta dr \qquad (2.14)$$

Here N, F and M equal, respectively, the resultant axial force, the resultant transverse shear force and the bending moment about the z-axis on a cross-section, and are, respectively, work conjugates of $u_\theta^0(\theta,t), u_r^0(\theta,t),$ and $\phi(\theta,t)$. These are depicted in Fig. 2. The other two quantities, P and R, introduced for convenience, do not have easy physical interpretations.

Substituting for stresses from equation (2.7) into equation (2.14) gives

$$F = b\int_{R_0-\frac{h}{2}}^{R_0+\frac{h}{2}} \tau_{r\theta} dr = b\int_{R_0-\frac{h}{2}}^{R_0+\frac{h}{2}} G(r,\theta)\left[\frac{1}{h^2 r}(h^2 - 4(r-R_0)^2)\left((u_r^0)' - u_\theta^0 + R_0\phi\right)\right] dr$$

$$R = b\int_{R_0-\frac{h}{2}}^{R_0+\frac{h}{2}} (r-R_0)^2 \tau_{r\theta} dr$$

$$= b\int_{R_0-\frac{h}{2}}^{R_0+\frac{h}{2}} G(r,\theta)\left[\frac{(r-R_0)^2}{h^2 r}(h^2 - 4(r-R_0)^2)\left((u_r^0)' - u_\theta^0 + R_0\phi\right)\right] dr$$

$$N = b\int_{R_0-\frac{h}{2}}^{R_0+\frac{h}{2}} \sigma_\theta dr$$

$$= b\int_{R_0-\frac{h}{2}}^{R_0+\frac{h}{2}} \frac{E(r,\theta)}{r}\left\{u_r^0 - U_0(u_1^0)' + (1+U_0)\left(u_\theta^0\right)' + (r - R_0 - R_0U_0)(\phi)'\right\} dr \qquad (2.15)$$

$$M = b\int_{R_0-\frac{h}{2}}^{R_0+\frac{h}{2}} (r-R_0)\sigma_\theta dr$$

$$= b\int_{R_0-\frac{h}{2}}^{R_0+\frac{h}{2}} \frac{(r-R_0)E(r,\theta)}{r}\left\{u_r^0 - U_0(u_1^0)' + (1+U_0)\left(u_\theta^0\right)'\right.$$

$$\left. + (r - R_0 - R_0U_0)(\phi)'\right\} dr$$

$$P = b\int_{R_0-\frac{h}{2}}^{R_0+\frac{h}{2}} U_0\sigma_\theta dr$$

$$= b\int_{R_0-\frac{h}{2}}^{R_0+\frac{h}{2}} \frac{U_0E(r,\theta)}{r}\left\{u_r^0 - U_0(u_1^0)' + (1+U_0)\left(u_\theta^0\right)' + (r - R_0 - R_0U_0)(\phi)'\right\} dr$$

Equation (2.15) expresses F, N, M, P and R in terms of the kinematic variables.

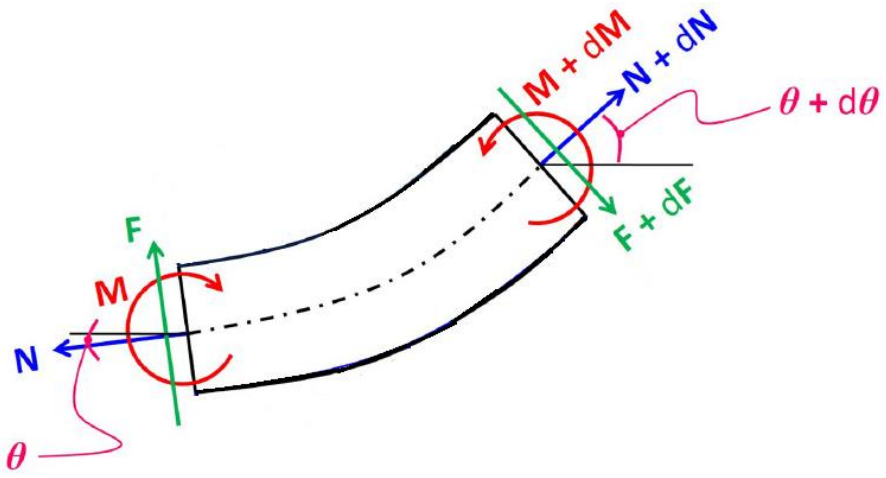

Figure 2 Free body diagram for a beam element [23].

Substituting from equations (2.11) and (2.13) into equation (2.9), we get

$$
\begin{aligned}
\delta A = b \int_{t_0}^{t_1} \int_{0}^{\theta_{tip}} \{ & A_1 \dot{u}_r^0 \delta \dot{u}_r^0 \\
& + \left[(A_1 + I_1 + 2K_1)\dot{u}_\theta^0 + (A_2 - R_0 A_1 - 2R_0 K_1 + K_2 - R_0 I_1)\dot{\phi} - (K_1 + I_1)\dot{u}_1^0 \right] \delta \dot{u}_\theta^0 \\
& + \left[(A_2 - R_0 A_1 - 2R_0 K_1 + K_2 - R_0 I_1)\dot{u}_\theta^0 \right. \\
& \left. + (A_3 + R_0^2 A_1 + R_0^2 I_2 - 2R_0 A_2 - 2R_0 K_2 + 2R_0^2 K_1)\dot{\phi} - (K_2 - R_0 K_1 - R_0 I_1)\dot{u}_1^0 \right] \delta \dot{\phi} \\
& + \left[-(K_1 + I_1)\dot{u}_\theta^0 - (K_2 - R_0 K_1 - R_0 I_1)\dot{\phi} + I_1 \dot{u}_1^0 \right] \delta \dot{u}_1^0 \, \} d\theta \, dt \\
& - b \int_{t_0}^{t_1} \int_{0}^{\theta_{tip}} \left[\left\{ N \delta u_r^0 - P \delta (u_1^0)' + (N + P) \delta \left(u_\theta^0 \right)' + (M - R_0 P) \delta (\phi)' \right\} \right. \\
& \left. + \frac{1}{h^2} (h^2 F - 4R) \left(\delta u_1^0 - \delta u_\theta^0 + R_0 \delta \phi \right) \right] d\theta \, dt = 0
\end{aligned}
\tag{2.16}
$$

Integrating with respect to θ terms like $\delta(\phi)'$ gives

$$
\begin{aligned}
&\int_{t_0}^{t_1}\int_{0}^{\theta_{tip}} \Big\{(N - F' + A_1\ddot{u}_r^0)\delta u_r^0 \\
&\quad + \Big[-N' - P' - F + \frac{4}{h^2}R + (A_1 + 2K_1 + I_1)\ddot{u}_\theta^0 \\
&\quad + (A_2 - R_0A_1 - 2R_0K_1 + K_2 - R_0I_1)\ddot{\phi} - \rho(K_1 + I_1)\ddot{u}_1^0\Big]\delta u_\theta^0 \\
&\quad + \Big[-M' + R_0P' + R_0F - \frac{4}{h^2}R_0R + (A_2 - R_0A_1 - 2R_0K_1 + K_2 - R_0I_1)\ddot{u}_\theta^0 \\
&\quad + (A_3 + R_0^2A_1 + R_0^2I_2 - 2R_0A_2 - 2R_0K_2 + 2R_0^2K_1)\ddot{\phi} - (K_2 - R_0K_1 - R_0I_1)\ddot{u}_1^0\Big]\delta\phi \\
&\quad + \Big[\Big(P' - \frac{4}{h^2}R\Big) - (K_1 + I_1)\ddot{u}_\theta^0 - (K_2 - R_0K_1 - R_0I_1)\ddot{\phi} + I_1\ddot{u}_1^0\Big]\delta u_1^0\Big\}\,d\theta dt \\
&\quad + \int_{t_0}^{t_1}\big[\{-P\delta u_1^0 + (N + P)\delta u_\theta^0 + (M - R_0P)\delta\phi\} + F\delta u_r^0\big]\Big|_0^{\theta_{tip}}\,dt \\
&\quad - \int_{0}^{\theta_{tip}} \{A_1\dot{u}_r^0\delta u_r^0 \\
&\quad + \big[(A_1 + I_1 + 2K_1)\dot{u}_\theta^0 + (A_2 - R_0A_1 - 2R_0K_1 + K_2 - R_0I_1)\dot{\phi} - (K_1 + I_1)(\dot{u}_1^0)\big]\delta u_\theta^0 \\
&\quad + \big[(A_2 - R_0A_1 - 2R_0K_1 + K_2 - R_0I_1)\dot{u}_\theta^0 \\
&\quad + (A_3 + R_0^2A_1 + R_0^2I_2 - 2R_0A_2 - 2R_0K_2 + 2R_0^2K_1)\dot{\phi} - (K_2 - R_0K_1 - R_0I_1)(\dot{u}_1^0)\big]\delta\phi \\
&\quad - \big[(K_1 + I_1)\dot{u}_\theta^0 + (K_2 - R_0K_1 - R_0I_1)\dot{\phi} - I_1\dot{u}_1^0\big]\delta u_1^0\big\}\Big|_{t_0}^{t_1}\,d\theta = 0
\end{aligned}
\tag{2.17}
$$

Using the fundamental lemma of the calculus of variations and assuming that δu_1^0 is also arbitrary, we obtain the following equations of motion and boundary conditions. We have not written initial conditions because they are not needed for studying free vibrations.

Governing equations:

$$
\begin{aligned}
&F' - N = A_1 \ddot{u}_r^0 \\
&N' + P' + F - \frac{4}{h^2} R \\
&\qquad = (A_1 + I_1 + 2K_1)\ddot{u}_\theta^0 + (A_2 - R_0 A_1 - 2R_0 K_1 + K_2 - R_0 I_1)\ddot{\phi} - \rho(K_1 + I_1)\ddot{u}_1^0 \\
&M' - R_0 P' - R_0 F + \frac{4}{h^2} R_0 R \\
&\qquad = (A_2 - R_0 A_1 - 2R_0 K_1 + K_2 - R_0 I_1)\ddot{u}_\theta^0 \\
&\qquad + (A_3 + R_0^2 A_1 + R_0^2 I_2 - 2R_0 A_2 - 2R_0 K_2 + 2R_0^2 K_1)\ddot{\phi} \\
&\qquad - (K_2 - R_0 K_1 - R_0 I_1)\ddot{u}_1^0 \\
&P' - \frac{4}{h^2} R = (K_1 + I_1)\ddot{u}_\theta^0 + (K_2 - R_0 K_1 - R_0 I_1)\ddot{\phi} - I_1 \ddot{u}_1^0
\end{aligned}
\tag{2.18}
$$

By substituting for P' from equation (2.18d) into equations (2.18b, c) we get the following three equations of motion for the three unknown fields, $u_\theta^0(\theta, t), u_r^0(\theta, t)$, and $\phi(\theta, t)$. These are supplemented by equation (2.5).

$$
\begin{aligned}
&F' - N = A_1 \ddot{u}_r^0 \\
&N' + F = (A_1 + K_1)\ddot{u}_\theta^0 + (A_2 - R_0 A_1 - R_0 K_1)\ddot{\phi} - K_1 \ddot{u}_1^0 \\
&M' - R_0 F = (A_2 - R_0 A_1 - R_0 K_1 + K_2)\ddot{u}_\theta^0 + (A_3 + R_0^2 A_1 - 2R_0 A_2 - R_0 K_2 + R_0^2 K_1)\ddot{\phi} \\
&\qquad - (K_2 - R_0 K_1)\ddot{u}_1^0
\end{aligned}
\tag{2.19}
$$

Boundary conditions at the ends $\theta = 0, \theta_{tip}$ require that

$$
\begin{aligned}
&\text{either } u_\theta \text{ or } N \text{ is prescribed} \\
&\text{either } \phi \text{ or } M \text{ is prescribed} \\
&\text{either } u_r \text{or } N \text{ is prescribed}
\end{aligned}
\tag{2.20}
$$

We write below equations for different boundary conditions at the edge $\theta = 0$.

Clamped: $u_r^0(0,t) = 0,\ u_\theta^0(0,t) = 0,\ \phi(0,t) = 0$ (2.21)

Hinged: $u_r^0(0,t) = 0,\ u_\theta^0(0,t) = 0,\ M(0,t) = 0$ (2.22)

Free: $F(0,t) = 0,\ N(0,t) = 0,\ M(0,t) = 0$ (2.23)

2.2. Free-Vibration analysis

For free vibrations, we assume that

$$\begin{aligned} u_r^0(\theta,t) &= e^{i\omega t}U_r^0(\theta) \\ \phi(\theta,t) &= e^{i\omega t}\Phi(\theta) \\ u_\theta^0(\theta,t) &= e^{i\omega t}U_\theta^0(\theta) \\ u_1^0(\theta,t) &= e^{i\omega t}U_1^0(\theta) \end{aligned} \tag{2.24}$$

Substituting these in equations (2.19) and (2.5) gives the following four homogeneous equations for finding the frequency ω and the corresponding mode shapes, $U_r^0(\theta), U_\theta^0(\theta), U_1^0(\theta)$ and $\Phi(\theta)$.

$$\begin{aligned} &F' - N + \omega^2 A_1 U_r^0(\theta) = 0 \\ &N' + F + \omega^2\left[(A_1 + K_1)U_\theta^0(\theta) + (A_2 - R_0A_1 - R_0K_1)\Phi(\theta) - K_1\, U_1^0(\theta)\right] = 0 \\ &M' - R_0F + \omega^2\big[(A_2 - R_0A_1 - R_0K_1 + K_2)U_\theta^0(\theta) \\ &\qquad + (A_3 + R_0^2A_1 - 2R_0A_2 - R_0K_2 + R_0^2K_1)\Phi(\theta) - (K_2 - R_0K_1)\, U_1^0(\theta)\big] = 0 \\ &\left(U_r^0(\theta)\right)' - U_1^0(\theta) = 0 \end{aligned} \tag{2.25}$$

2.3.Generalized Differential Quadrature Method

We use the generalized differential quadrature method (GDQM) [26] to numerically solve equations (2.25) for frequencies and mode shapes. In the GDQM, the derivative of a function with respect to a coordinate direction is expressed as a weighted linear sum of values of the function at all mesh points along that direction. That is,

$$u^{(m)}(\theta_i) = \sum_{j=1}^{n} c_{ij}^{(m)}\, u(\theta_j), \qquad \text{for } i = 1,2,\dots,n \tag{2.26}$$

where

$$\begin{aligned} c_{ij}^{1} &= \frac{M^{(1)}(\theta_i)}{(\theta_i - \theta_j) M^{(1)}(\theta_j)}, \qquad \text{for } i \neq j \\ c_{ii}^{1} &= \frac{M^{(2)}(\theta_i)}{2M^{(1)}(\theta_i)}, \qquad \text{for } i = j \end{aligned} \tag{2.27}$$

where

$$\begin{aligned} M^{(1)}(\theta_i) &= \prod_{j=1, j\neq i}^{n} (\theta_i - \theta_j) \\ M^{(2)}(\theta) &= dM^{(1)}(\theta)/d\theta \end{aligned} \tag{2.28}$$

We note that one could alternatively use the smooth symmetric particle hydrodynamics (SSPH) method [31, 32] that expresses the first and the second derivatives at a point in terms of values of the function at neighboring points.

We use the Chebyshev-Gauss-Lobbatto (CGL) grid on the domain [0, θ_{tip}] in which the location θ_i of a point in the n-point grid is given by

$$\theta_i = \frac{1}{2}\left[1 - cos\left(\frac{i-1}{n-1}\pi\right)\right]\theta_{tip} \tag{2.29}$$

In Figure 3 we display the locations of the grid points for $\theta_{tip} = 180°, n = 23$.

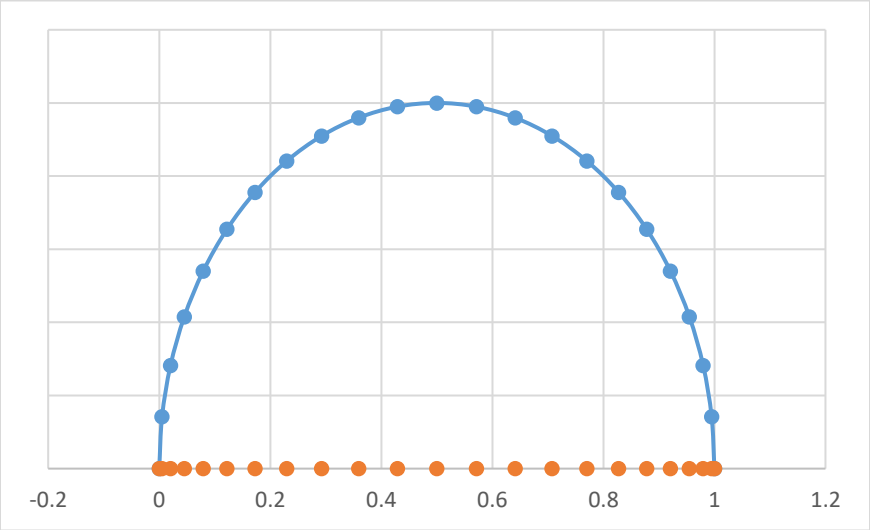

Figure 3 Chebyshev-Gauss-Lobbatto (CGL) grid points for n=23

Using the summation convention, i.e., a repeated index implies summation over the range of the index, we write equations (2.25) as

$$c_{ij}^1 F(\theta_j) - N(\theta_i) + \omega^2 A_1 U_r^0(\theta_i) = 0$$

$$c_{ij}^1 N(\theta_j) + F(\theta_i) + \omega^2(A_1 + K_1)U_\theta^0(\theta_i) + \omega^2(A_2 - R_0A_1 - R_0K_1)\Phi(\theta_i) - \omega^2 K_1 U_1^0(\theta_i) = 0$$

$$c_{ij}^1 M(\theta_j) - R_0 F(\theta_i) + \omega^2(A_2 - R_0A_1 - R_0K_1 + K_2)U_\theta^0(\theta_i) + \omega^2(A_3 + R_0^2A_1 - 2R_0A_2 - R_0K_2 + R_0^2K_1)\Phi(\theta_i) - \omega^2(K_2 - R_0K_1)U_1^0(\theta_i) = 0 \tag{2.30}$$

$$c_{ij}^1 U_r^0(\theta_j) - U_1^0(\theta_i) = 0$$

We regard equations (2.15a, c and d) and (2.30) as 7 equations for the 7 unknowns, namely, *F*, *N*, *M*, $U_r^0(\theta), U_\theta^0(\theta), U_1^0(\theta)$ and $\Phi(\theta)$. We find natural frequencies ω of the beam by first modifying these equations to satisfy boundary conditions that eliminate the rigid body modes (except for a free-free beam) and then setting the determinant of the coefficient matrix of the system of homogeneous algebraic equations equal to zero. For each frequency so found, we compute the corresponding eigenvector to get the mode shape that is normalized by setting equal to 1 its maximum value. We have developed an in-house MATLAB code to analyze the eigenvalue problem.

2.4. Material gradation

We consider three gradation of the material properties of which only one has variation in both directions. For gradation of material property, *Q*(r) (e.g., E, G and ρ), in the radial or the thickness direction we assume either the affine gradation

$$Q(r) = Q_{out} - (Q_{out} - Q_{in})\left(\frac{1}{2} - \frac{r - R_0}{h}\right) \tag{2.31}$$

or the exponential

$$Q(r) = Q_{in}\left(\frac{r}{r_{in}}\right)^2 exp\left\{\frac{\left[ln\left(\frac{Q_{out}}{Q_{in}}\right) - 2ln\left(\frac{r_{out}}{r_{in}}\right)\right]\left[\left(\frac{r}{r_{in}}\right) - 1\right]}{\left(\frac{r_{out}}{r_{in}}\right) - 1}\right\} \tag{2.32}$$

The subscripts “in” and “out” signify, respectively, values of the quantity on the inner and the outer surfaces of the beam.

For bi-directional gradation of the material properties in both the radial and the circumferential directions we assume

$$Q(r, \theta) = Q^* f(r) g(\theta) \tag{2.33}$$

were Q^* represent a constant property of the material, and $f(r)$ and $g(\theta)$ are non-dimensional functions representing gradations along the radial and the circumferential directions, respectively. For numerical examples we choose the following functions that are the same as those in [23].

$$f(r) = 1 + \left(\frac{Q_{in}}{Q_{out}} - 1\right)\left(\frac{1}{2} - \frac{r - R_0}{h}\right)^{\lambda_r}, \qquad (with\ Q^* = Q_{out}) \tag{2.34}$$

$$g(\theta) = exp(\lambda_\theta \theta) \tag{2.35}$$

Here θ is in radians, and λ_θ and λ_r are non-dimensional parameters (also called gradation indices) dictating the properties variation along the radial and the circumferential directions.

In this work, unless otherwise mentioned, the gradation indices are chosen to be $\lambda_r = 1, \lambda_\theta = -0.25$ for which we have exhibited in Fig. 4 the spatial variation of $Q(r, \theta)$.

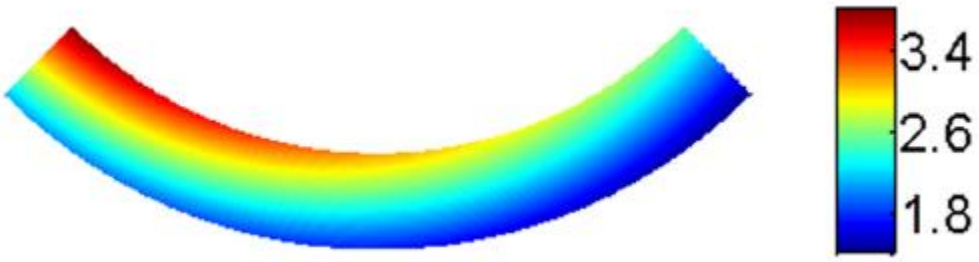

Figure 4 Variation of Q/Q in a bi-directional FGM circular beam with $\lambda_r = 1, \lambda_\theta = -0.25$ [23]*

3. Results and Discussion

3.1. Verification and Convergence of the Solution

We verify the accuracy and the convergence of the developed algorithm by comparing frequencies computed for a homogeneous circular beam and then for a FGM beam with their literature values. For clamped-clamped and hinged-hinged arches, and different number, n, of grid points, we list in Tables 1 and 2 the first five non-dimensional frequencies, $c = \omega {R_0}^2 {\theta_{tip}}^2 \sqrt{\mu/EI}$, where μ is the mass per unit length (=ρbh), and I is the moment of inertia of the cross-section about the z-axis (=$bh^3/12$). These results establish that 21 grid points provide converged values of the first 5 frequencies, and their values agree well with those reported in [25] that used a different higher order beam theory. As expected, the 1st frequency converges much faster than the 5th frequency. For R_0/h = 50 and 100, the first (fifth) frequency of the hinged-hinged beam is about 52% (76%) of that for the clamped-clamped beam. For R_0/h = 10, these ratios are, respectively, 52% and 95%. Results for $R_0/h = 10$ are not given in [25].

Table 1 Non-dimensional frequencies, $c = \omega {R_0}^2 {\theta_{tip}}^2 \sqrt{\mu/EI}$, for uniform, homogeneous and monolithic clamped-clamped (hinged-hinged) 180° *circular arches*

R_0/h	N	ω_1	ω_2	ω_3	ω_4	ω_5
100	13	43.27(22.37)	95.04(68.33)	175.4(137.9)	296.1(224.0)	445.9(340.1)
	15	43.26(22.37)	95.23(68.32)	176.9(137.9)	268.3(225.3)	383.9(334.6)
	19	43.26(22.37)	95.22(68.32)	176.8(137.9)	171.3(225.1)	392.1(334.7)
	21	43.26(22.37)	95.22(68.32)	176.8(137.9)	271.4(225.1)	392.4(334.7)
	23	43.26(22.37)	95.22(68.32)	176.8(137.9)	271.4(225.1)	392.3(334.7)
	[25]	43.17(22.35)	94.76(68.16)	175.7(137.4)	268.5(223.7)	387.7(332.1)
	Diff. (%)	0.2(0.01)	0.5(0.2)	0.6(0.4)	1(0.6)	1.1(0.8)

50	13	43.24(22.37)	94.91(68.26)	175.1(137.8)	295.0(223.7)	443.4(339.4)
	15	43.24(22.37)	95.10(68.28)	176.6(137.8)	267.5(225.0)	382.7(334.0)
	19	43.24(22.37)	95.09(68.28)	176.5(137.8)	270.5(224.8)	390.8(334.0)
	21	43.24(22.37)	95.09(68.28)	176.5(137.8)	270.6(224.8)	391.1(334.0)
	23	43.24(22.37)	95.09(68.28)	176.5(137.8)	270.6(224.8)	391.0(334.0)
	[25]	42.87(22.28)	93.27(67.67)	172.3(135.9)	258.5(219.3)	372.8(324.0)
	Diff. (%)	0.8(0.4)	1.9(0.9)	2.4(1.4)	4.4(2.4)	4.7(3.0)
10	13	42.4(22.24)	90.92(67.21)	166.3(134.2)	251.8(212.5)	355.4(330.6)
	15	42.4(22.24)	91.08(67.20)	167.4(134.2)	239.8(213.6)	350.0(330.8)
	19	42.4(22.24)	91.07(67.20)	167.3(134.2)	241.3(213.6)	348.8(330.5)
	21	42.4(22.24)	91.07(67.20)	167.3(134.2)	241.3(213.6)	348.9(330.5)
	23	42.4(22.24)	91.07(67.20)	167.3(134.2)	241.3(213.6)	348.9(330.5)

For the FGM beam, we compare results computed from our code with those of Filipich and Piovan [27] who considered a beam with the inner and the outer surfaces made, respectively, of steel and alumina having the following values of material parameters.

$$E_{St} = 214\ GPa, G_{St} = 82.2\ GPa, \rho_{St} = 7800\ \frac{Kg}{m^3}$$
$$E_{Al_2O_3} = 390\ GPa, G_{Al_2O_3} = 137\ GPa, \rho_{Al_2O_3} = 3200\ \frac{Kg}{m^3} \quad (3.1)$$

For clamped-clamped and cantilever FGM beams of $R_0 = 0.5\,m, h = 0.05\,m,$ and $\theta_{tip} = 1\,rad$, we compare in Table 2 the presently computed natural frequencies with those of [27].

Table 2 Natural frequency (Hz) of the clamped-clamped (cantilever) circular arch with linear radial gradation of material properties

N	ω_1	ω_2	ω_3	ω_4	ω_5
13	2390(241.4)	3628(1268)	7069(3567)	7726(4450)	11150(7178)
15	2390(241.4)	3628(1268)	7089(3540)	7726(4442)	11170(7132)
19	2390(240.4)	3628(1268)	7089(3542)	7726(4443)	11170(7136)
21	2390(240.4)	3628(1268)	7089(3542)	7726(4443)	11170(7136)
23	2390(240.4)	3628(1268)	7089(3542)	7726(4443)	11170(7136)
Ref. [27]	2367(241.40)	3431(1245)	6497(3419)	7702(4397)	(Not Calculated)
Diff %	1.0(0.4)	5.3(1.8)	8.3(3.4)	0.3(1.0)	

We see that the presently computed first five natural frequencies agree with those reported in [27] deduced by using the Timoshenko beam theory as the maximum difference between any two sets of results is 8.3% for the third natural frequency for the clamped-clamped beam. For this beam, 15 points in equation (2.28) provide converged values of the first five frequencies. The first (fifth) frequency of the cantilever beam is about 10% (64%) of that for the clamped-clamped beam

3.2. Frequencies of the bi-directional FGM beam

For the steel/alumina bi-directionally graded half-circular beam with material properties given by equations (2.33) – (2.35) and $R_0 = 0.5\ m$, $h = 0.05\ m$ and $\theta_{tip} = \pi\ rad$ we list in Table 3 for different edge conditions converged frequencies by taking n = 23 in equation (2.28).

Table 3 Natural frequency (Hz) of half-circular beam with bi-directional gradation of material properties with radius $R_0 = 0.5\ m$, thickness $h = 0.05\ m$ and opening angle $\theta_{tip} = \pi\ rad$

Boundary condition	λ_θ	ω_1	ω_2	ω_3	ω_4	ω_5
Clamped-Clamped	0	290.6	625.2	1156	1675	2317
	0.25	290.8	625.6	1155.8	1674.32	2301
	1	294.4	632.2	1149	1661	2204
	2	313.2	654.7	1140	1635	2146
Hinged-Hinged	0	150.6	453.4	909.5	1450	2148
	0.25	149.8	453.5	909.3	1450	2138
	1	138.2	455.4	906.2	1445	2066
	2	107.3	465.1	905.7	1437	1990
Cantilever	0	29.40	91.78	311.7	498.2	687.8
	0.25	23.23	78.32	293.8	560.6	671.5
	1	10.79	45.64	241.0	313.6	629.1
	2	3.495	19.32	96.00	172.3	590.2
Free-Free	0	123.0	351.7	730.8	1240	1870
	0.25	124.1	352.7	731.8	1241	1871

1	139.4	368.2	746.7	1255	1885
2	187.6	417.6	794.4	1302	1931

The effects of radial and circumferential gradation of material properties for a half-circular beam with clamped-clamped boundary conditions are shown in Figure (5), where $\alpha = \omega_1 {R_0}^2 {\theta_{tip}}^2 \sqrt{\mu_{Al_2O_3}/E_{Al_2O_3} I}$ represents the dimensionless fundamental frequency parameter. Thus, for a fixed value of λ_θ, α monotonically increases with an increase in λ_r, and α only depends upon the magnitude of λ_θ.

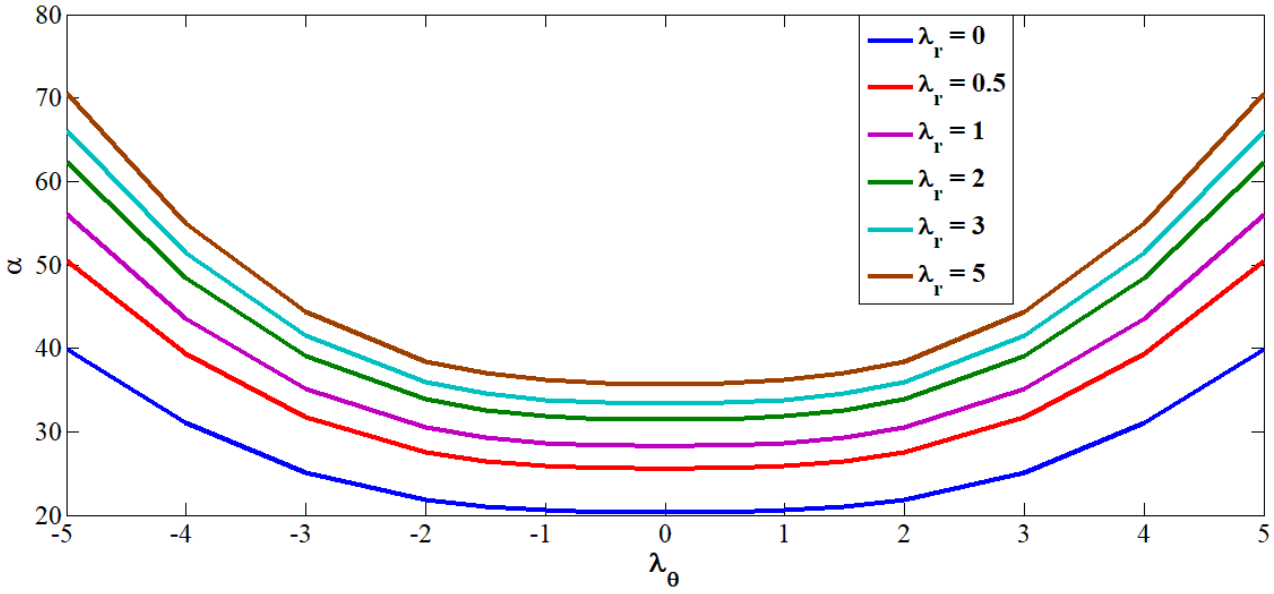

Figure 5 Variation of the fundamental frequency with the gradation indices for a clamped-clamped half-circular bi-directional FGM beam

In order to see how frequencies of the FGM beam compare with those of the monolithic steel and alumina beams we list below their frequencies.

Table 4 Natural frequencies of steel (alumina) beam of radius $R_0 = 0.5\ m$, thickness $h = 0.05\ m$ and opening angle $\theta_{tip} = 1\ rad$

Material	$B.C$	ω_1	ω_2	ω_3	ω_4	ω_5

Steel(Alumina)	Clamped-Clamped	1679(3538)	2396(5051)	4494(9472)	5272(11110)	6822(14380)
	Cantilever	170.3(359.1)	892.8(1882)	2381(5019)	3106(6548)	4635(9770)
	Hinged-Hinged	1542(3249)	1650(3478)	3652(7698)	5284(11140)	6083(12820)
	Free-Free	1007(2123)	2663(5612)	4893(10314)	5483(11556)	7493(15793)

Table 5 Natural frequencies of steel (alumina) for $(R_0, h, \theta_{tip}) = (0.5\ m, 0.05\ m, \pi\ rad)$

	$B.C$	ω_1	ω_2	ω_3	ω_4	ω_5
Steel(Alumina)	Clamped-Clamped	206.0(434.1)	441.8(931.8)	809.9(1707)	1168(2461)	1684(3548)
	Cantilever	20.87(43.99)	65.59(138.2)	222.0(468.0)	488.9(1030)	838.3(1767)
	Hinged-Hinged	107.9(227.3)	325.4(685.8)	648.5(1367)	1029(2168)	1593(3357)
	Free-Free	88.22(185.9)	253.3(534.0)	525.3(1107)	887.4(1870)	1331(2805)

It is evident that a natural frequency of the FGM beam is bounded by that of the monolithic beams.

We have not listed in Tables 3-5 the null natural frequencies for free-free beams corresponding to the infinitesimal rigid body modes given by [33]

$$\begin{bmatrix} u_r \\ u_\theta \end{bmatrix} = \begin{bmatrix} c^1 \cos(\theta) + c^2 \sin(\theta) \\ -c^1 \sin(\theta) + c^2 \cos(\theta) + d^3 r \end{bmatrix} \tag{3.2}$$

where c^1, c^2, and d^3 are constants. One can easily verify that displacements (3.2) correspond to null strains.

3.3. Mode transition

For different values of θ_{tip} of clamped-clamped and hinged-hinged monolithic and FGM circular beams, we have plotted in Figure 6 the variation of the first two non-dimensional frequencies

$$\beta = \omega R^2 \sqrt{\mu_{out}/E_{out} I} \tag{3.3}$$

It is clear that the two frequencies are very close to each other for $\theta_{tip} = 75°\,(60°)$ for clamped-clamped (hinged-hinged) beam irrespective of the material gradation.

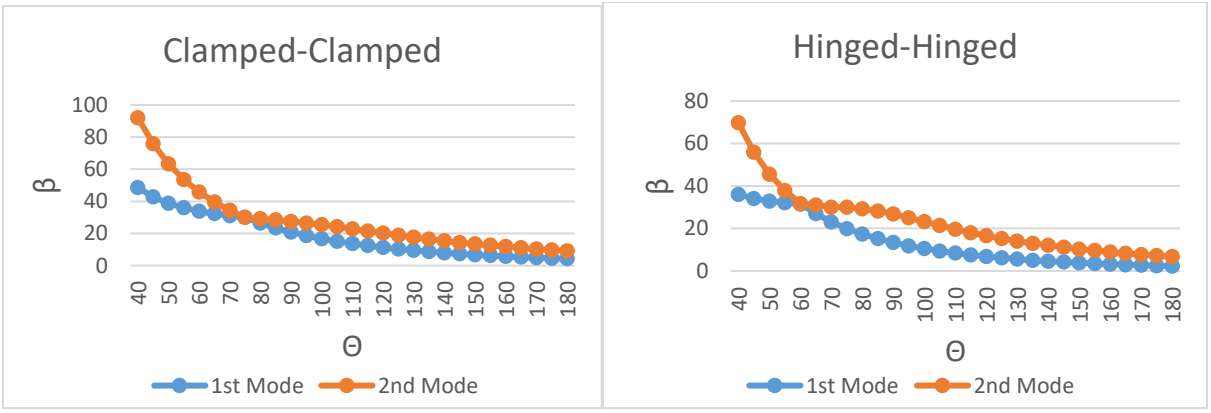

(a)

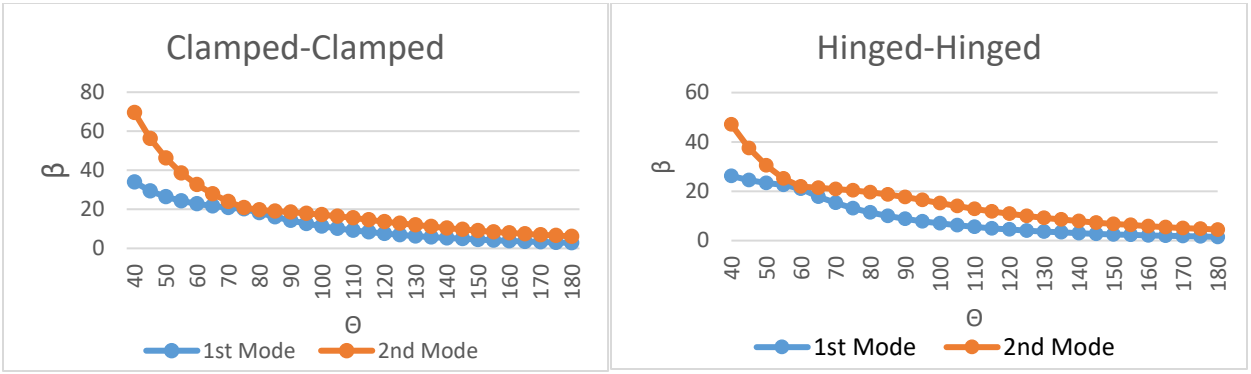

(b)

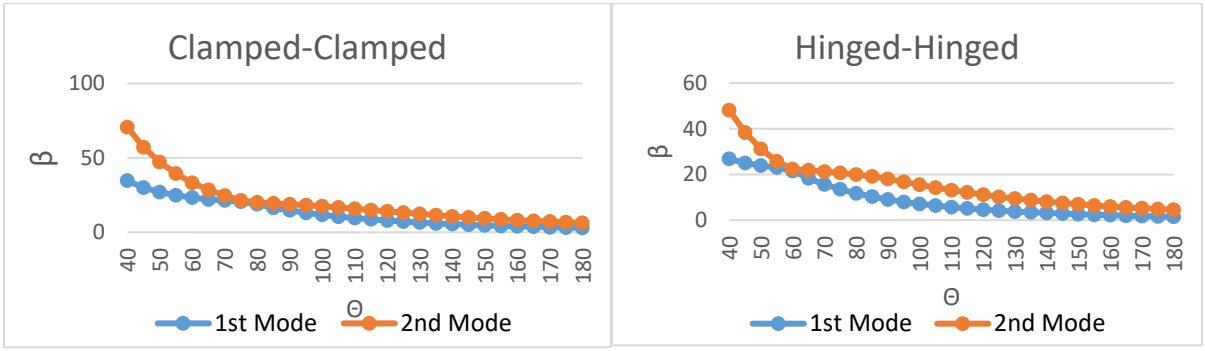

(c)

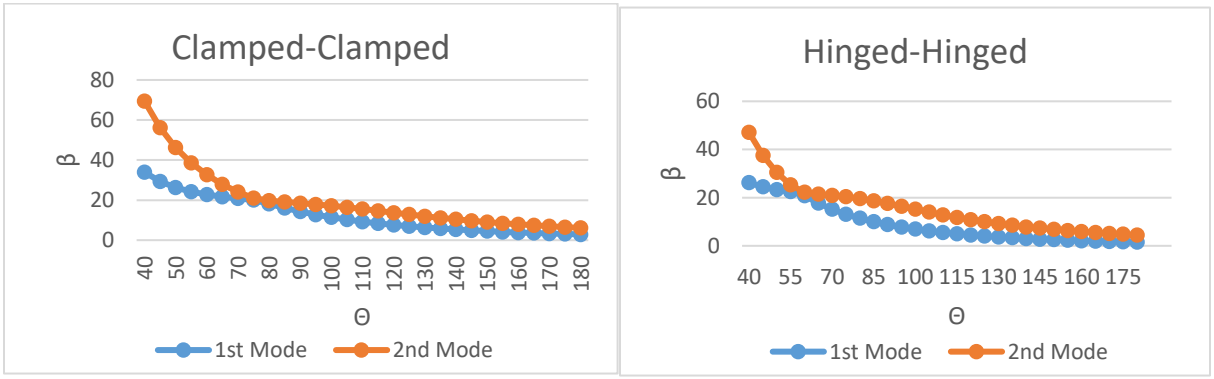

(d)

Figure 6 Variation with the opening angle of the first two natural non-dimensional frequencies for (left) clamped-clamped and (right) hinged-hinged circular arches composed of (a) homogeneous material, (b) linear radially graded FGM, (c) exponential radially graded FGM, and (d) bi-directionally graded FGM.

For clamped-clamped beams with $\theta_{tip} = 70°$ and $85°$ and exponential radial gradation of the material properties, we have plotted in Figure 7 the first two mode shapes. No scales are included along the horizontal and the vertical axes because the mode shapes have been normalized by setting the maximum radial displacement equal to 1. Thus, they provide only qualitative picture of the two mode shapes. It is clear that the two mode shapes are interchanged as θ_{tip} passes through the mode-transition value.

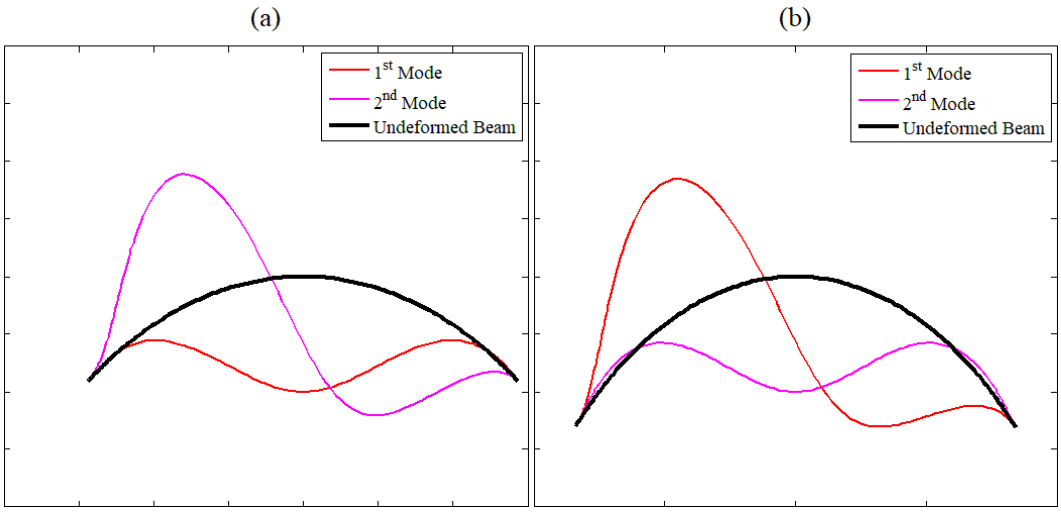

Figure 7 Deformed configuration clamped-clamped circular beam with exponential radially gradation of material properties. (a) $\theta_{tip} = 70°$ *(b)* $\theta_{tip} = 85°$

3.4. Mode Shapes

By using the afore-stated normalization for mode shapes, we have exhibited in Figure 8 the first four mode shapes for clamped-clamped, hinged-hinged and free-free semi-circular FGM beams for exponential radial and bi-directional gradation of material properties. It is clear that bi-directionally grading the material properties affects the mode shapes.

Exponential Radial Material Gradation

Bi-directional Material Gradation ($\lambda_\theta = 1$)

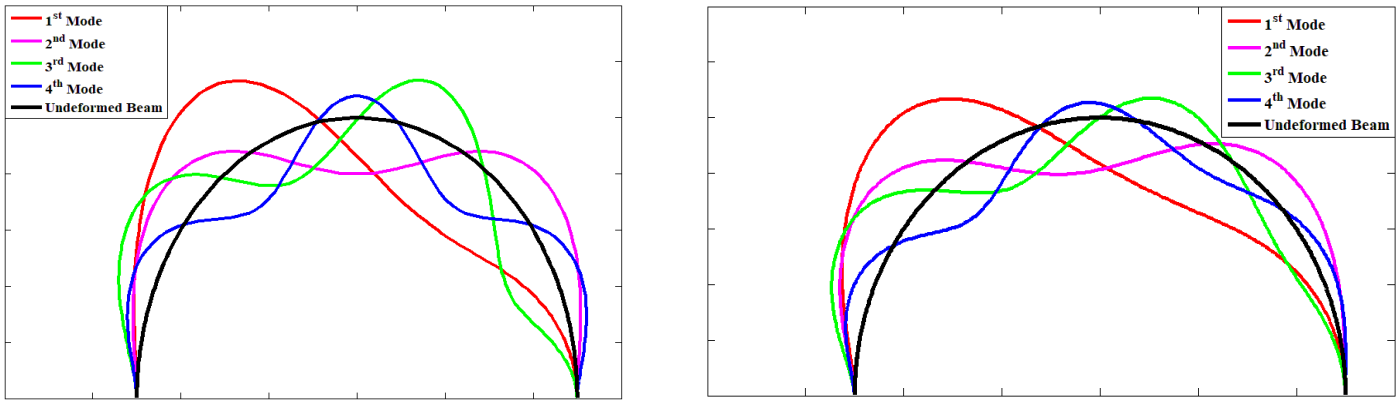

(a)

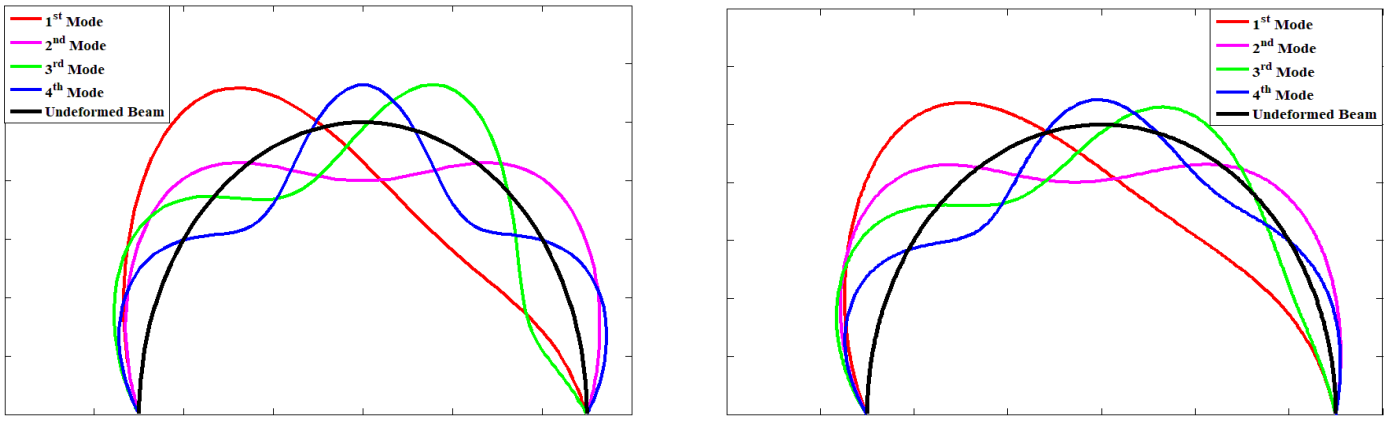

(b)

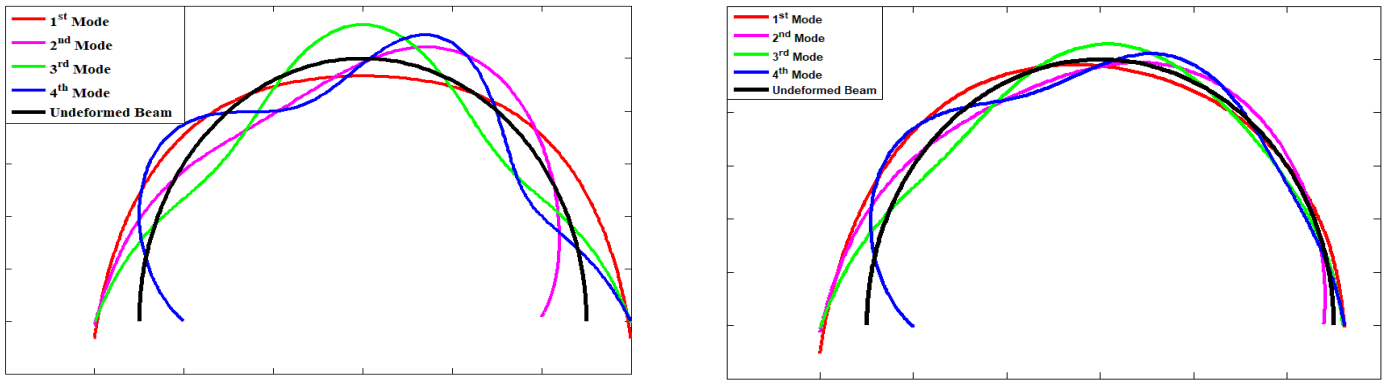

(c)

Figure 8 First four mode shapes for semi-circular (left) exponential radial and (right) bi-directional gradation of (a) clamped-clamped, (b) hinged-hinged, and (c) free-free FGM beams ($\theta_{tip} = \pi\ rad$)

We have plotted in Figure 9, for various edge conditions, the variation along the circumferential direction of $U_r^0(\theta), U_1^0(\theta), U_\theta^0(\theta)$ and $\Phi(\theta)$ (i.e., the mid-surface radial displacement, the slope of the mid-surface displacement, the circumferential displacement, and the angle of rotation, respectively). These have been normalized to have the maximum value 1 (in appropriate units) at a point in $[0, \pi]$. The variation of $U_r^0(\theta)$ indicates how the beam deforms in the lateral direction, and that of $U_\theta^0(\theta)$ is a measure of stretching along the circumferential direction. We see that the edge conditions strongly influence the variation of $U_r^0(\theta)$ and the point where the maximum value 1 of $U_1^0(\theta)$ occurs.

Exponential radial gradation

Clamped-Clamped

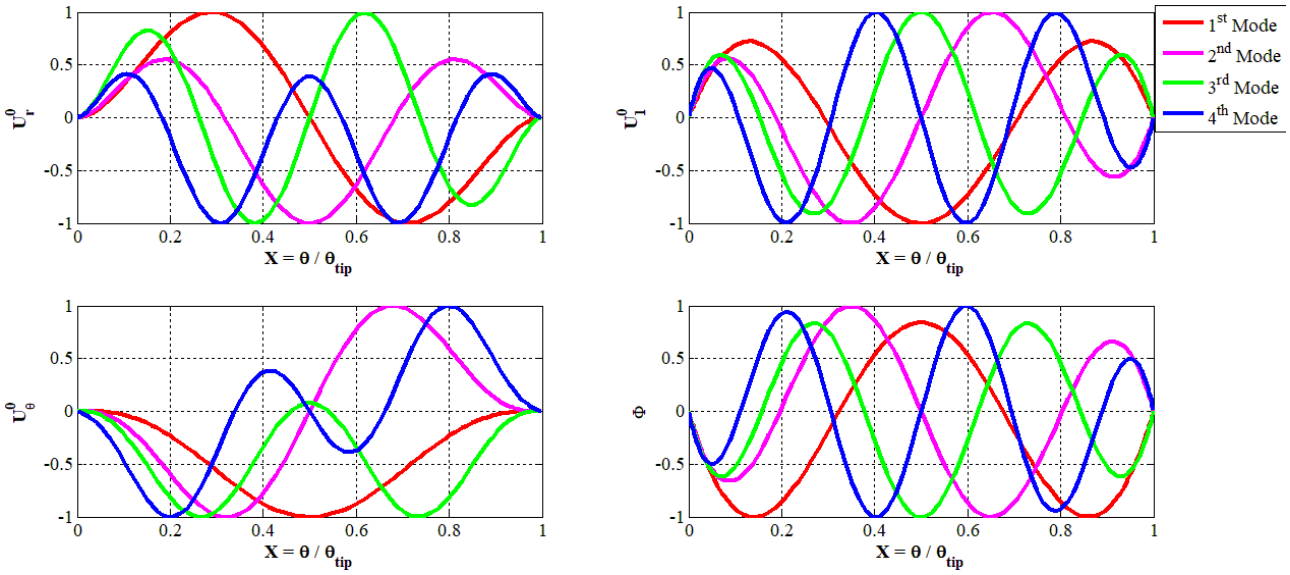

Hinged-Hinged

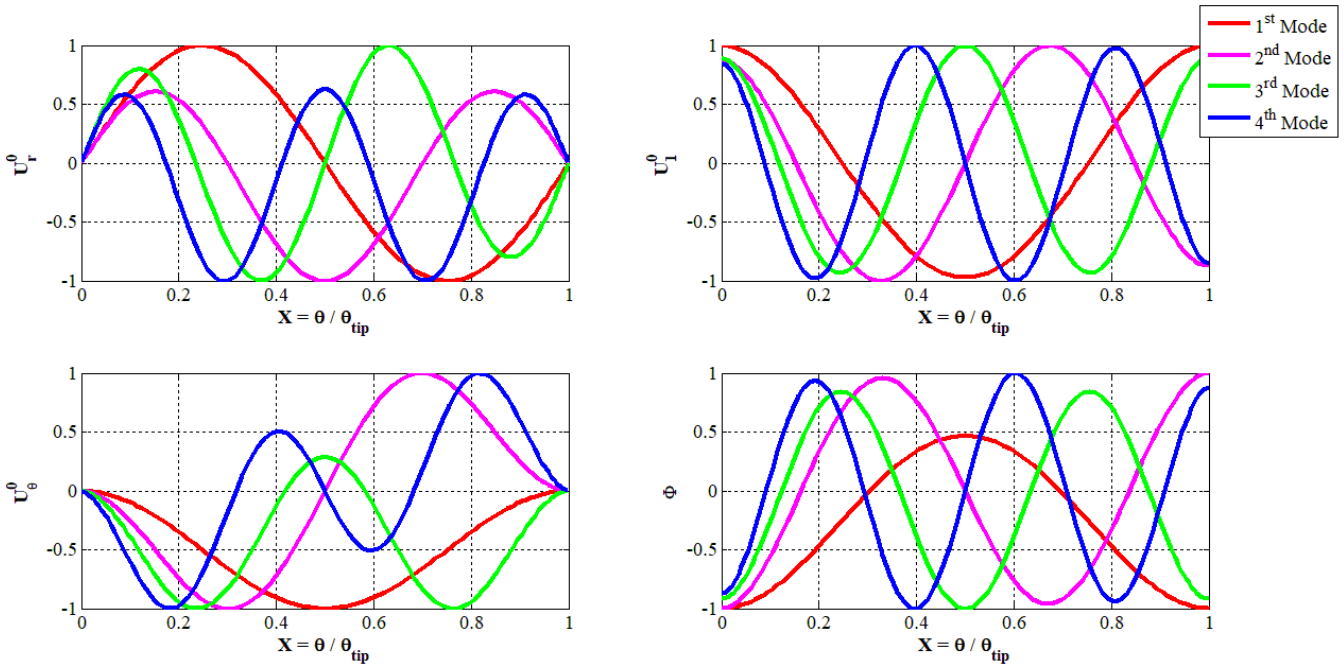

Free-Free

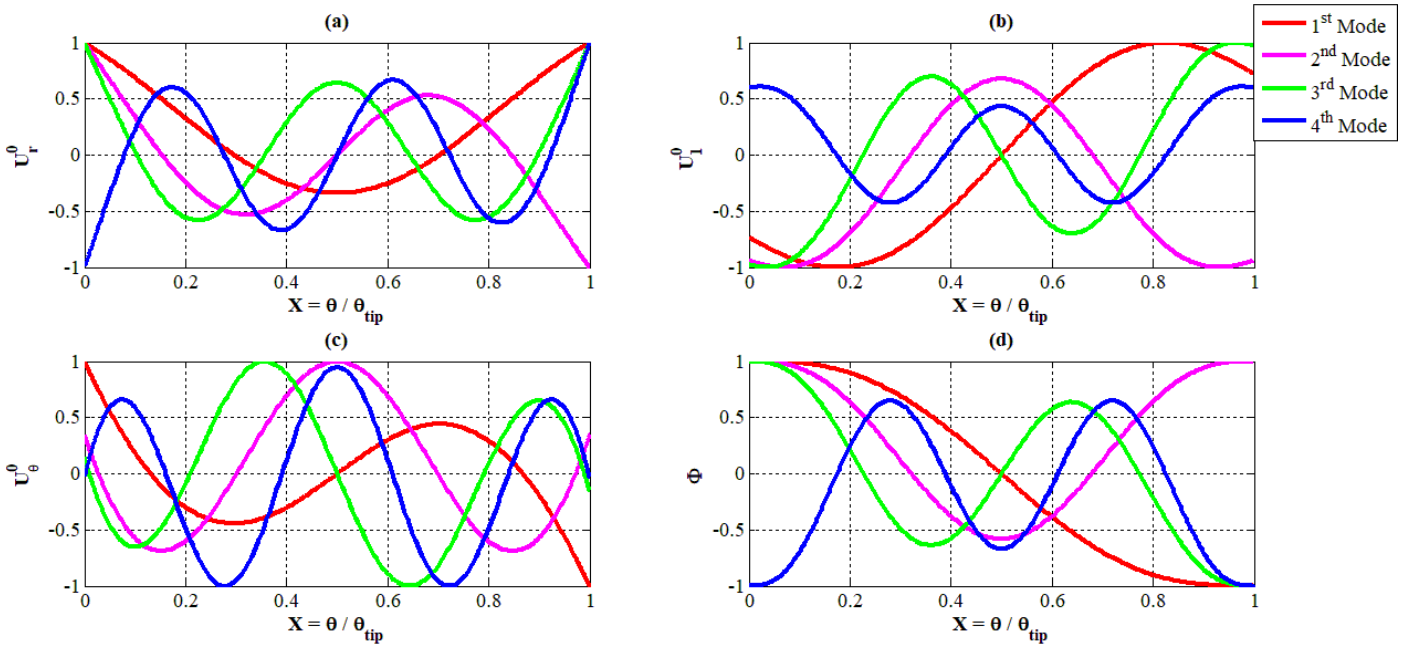

Bi-directional gradation ($\lambda_\theta = 1$)

Clamped-Clamped

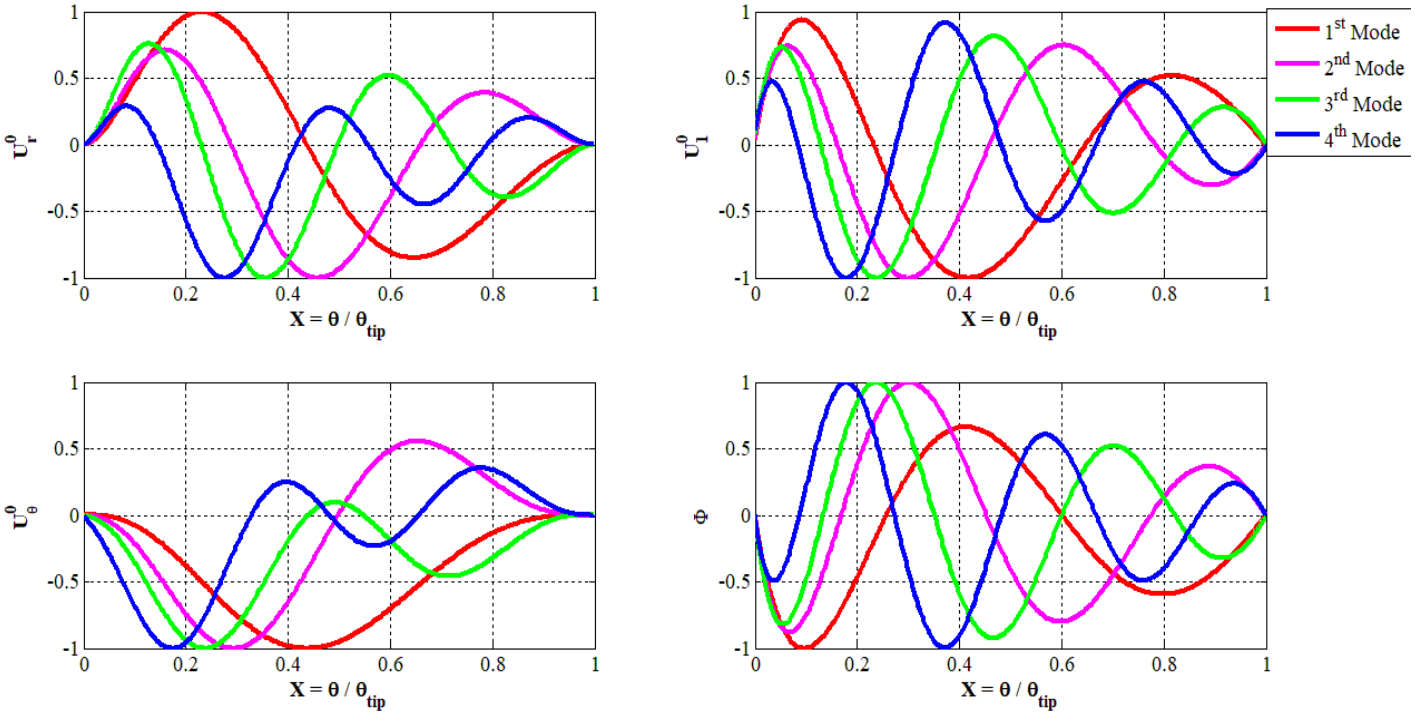

Hinged-Hinged

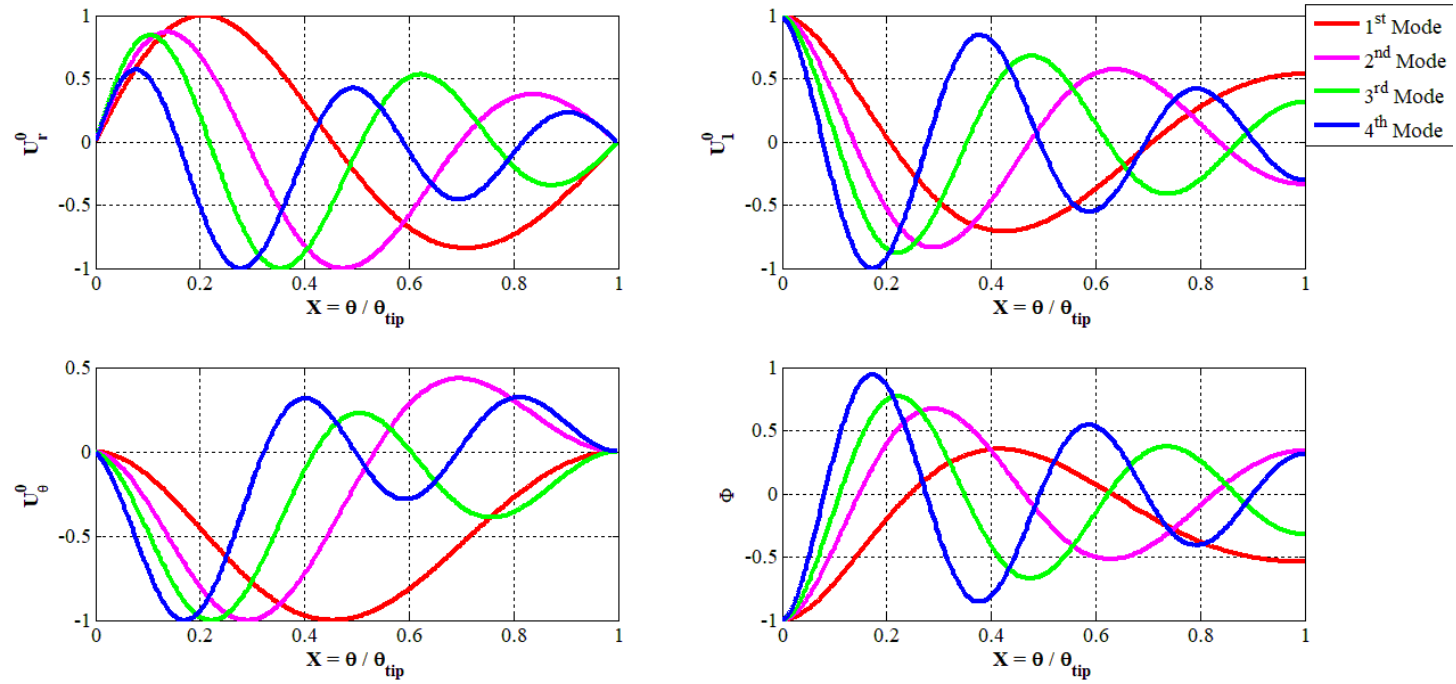

Free-Free

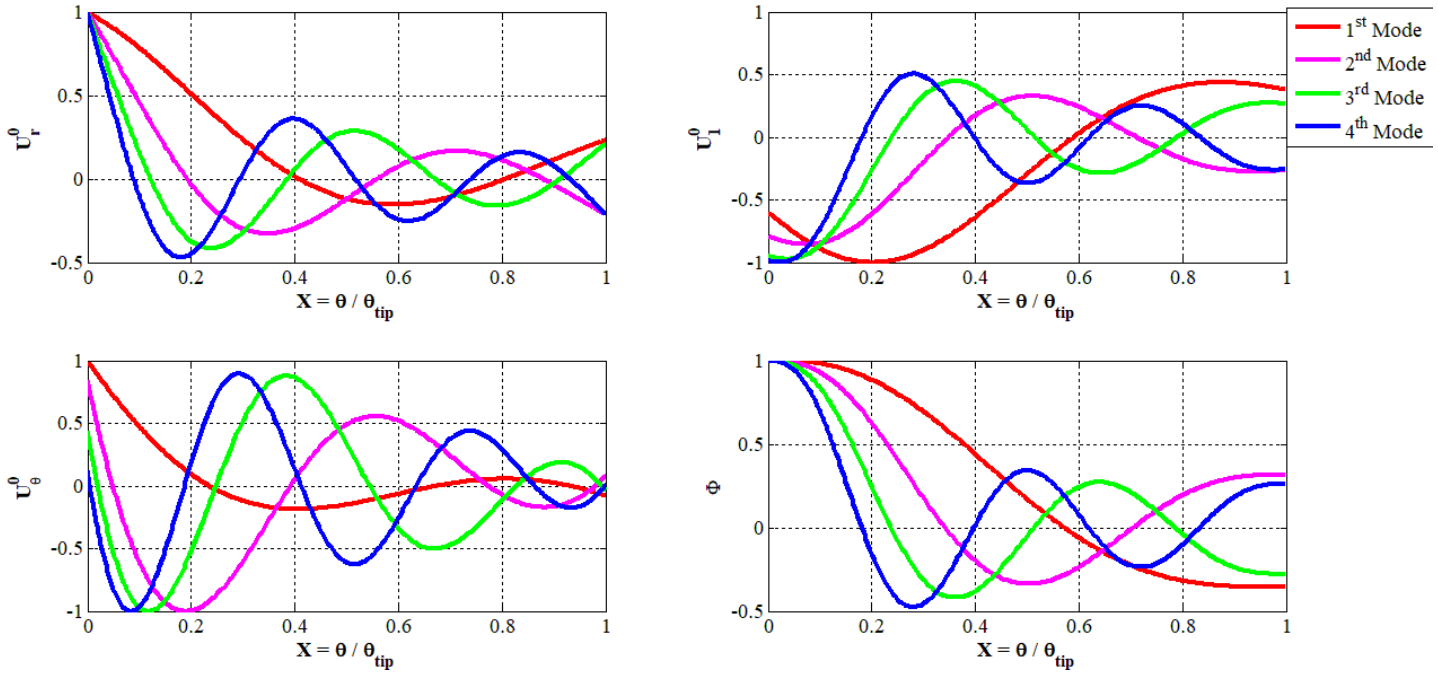

Figure 9 Variation with the angular position of the normalized displacements for the first four mode shapes of a semi-circular FGM beam ($\theta_{tip} = \pi\ rad$)

The variations of stress resultants along the beam length for the four mode shapes corresponding to different edge conditions are exhibited in Figure 10. These have been normalized to have the maximum value 1 (appropriate units) at a point in [0, π]. The mode shapes for the stress resultants do not qualitatively agree with those for any one of the four generalized displacements, $U_r^0(\theta), U_\theta^0(\theta), U_1^0(\theta)$ and $\Phi(\theta)$ because their expressions involve a combination of derivatives of displacements.

Exponential radial gradation

Clamped-Clamped

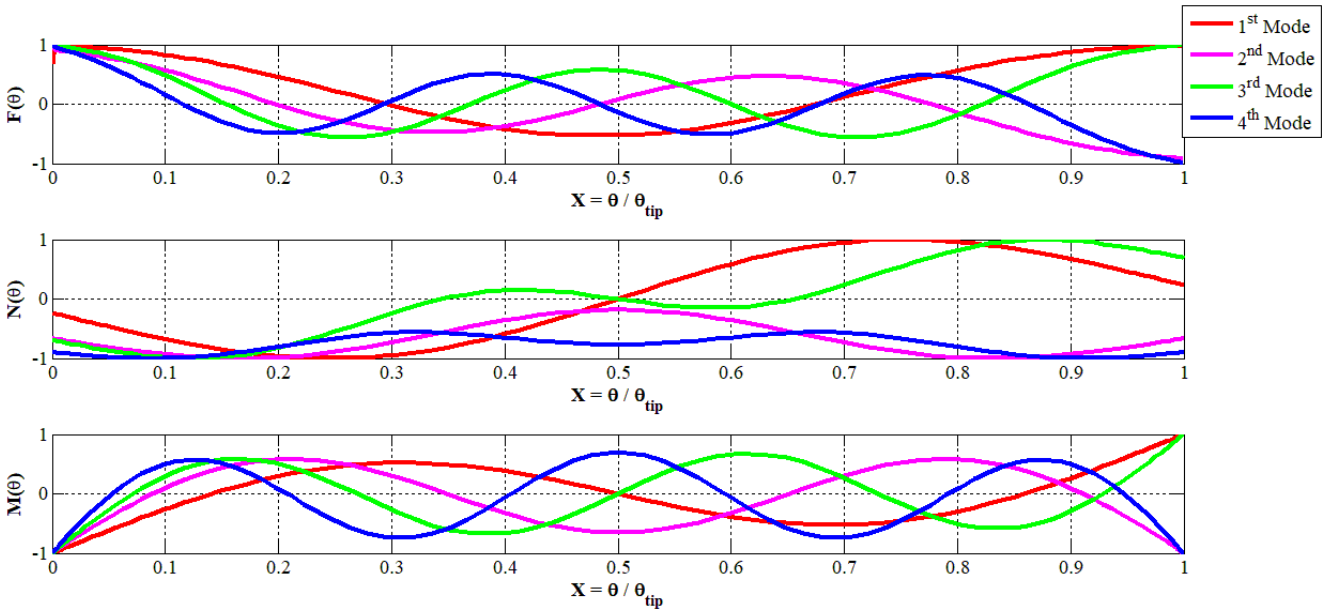

Hinged-Hinged

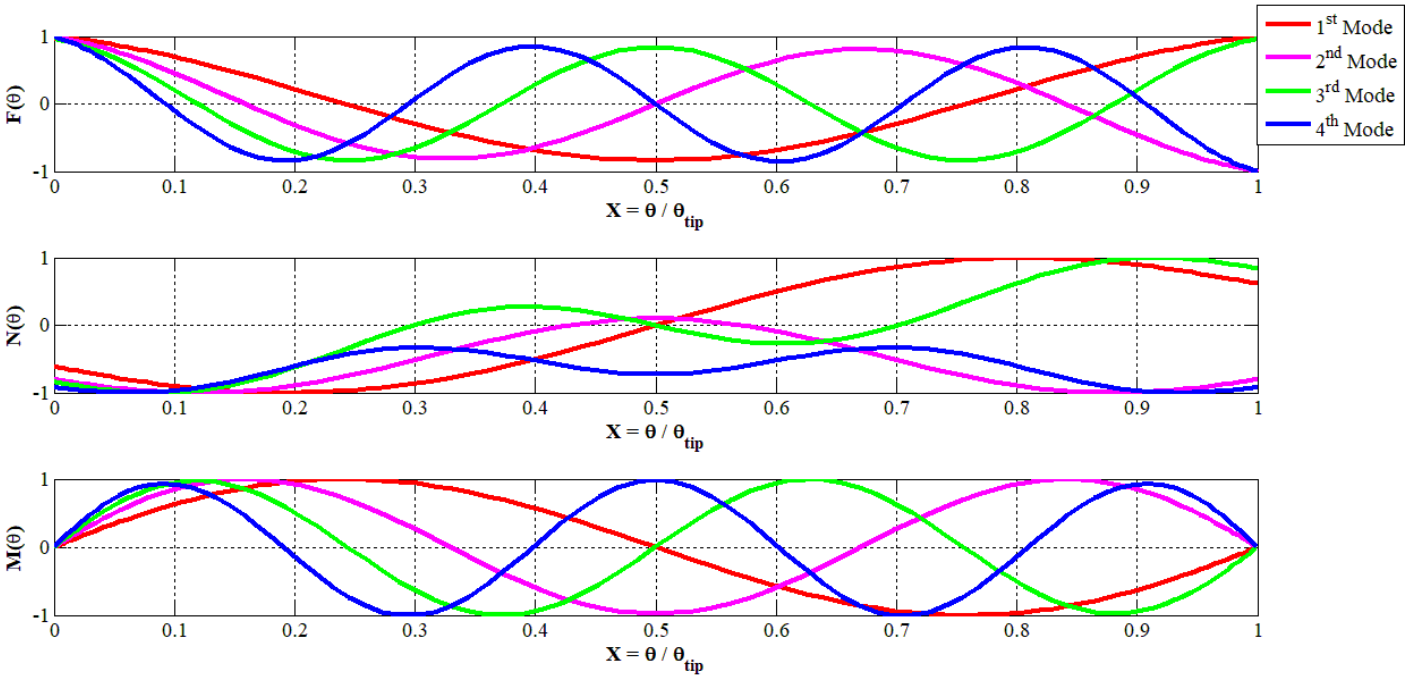

Free-Free

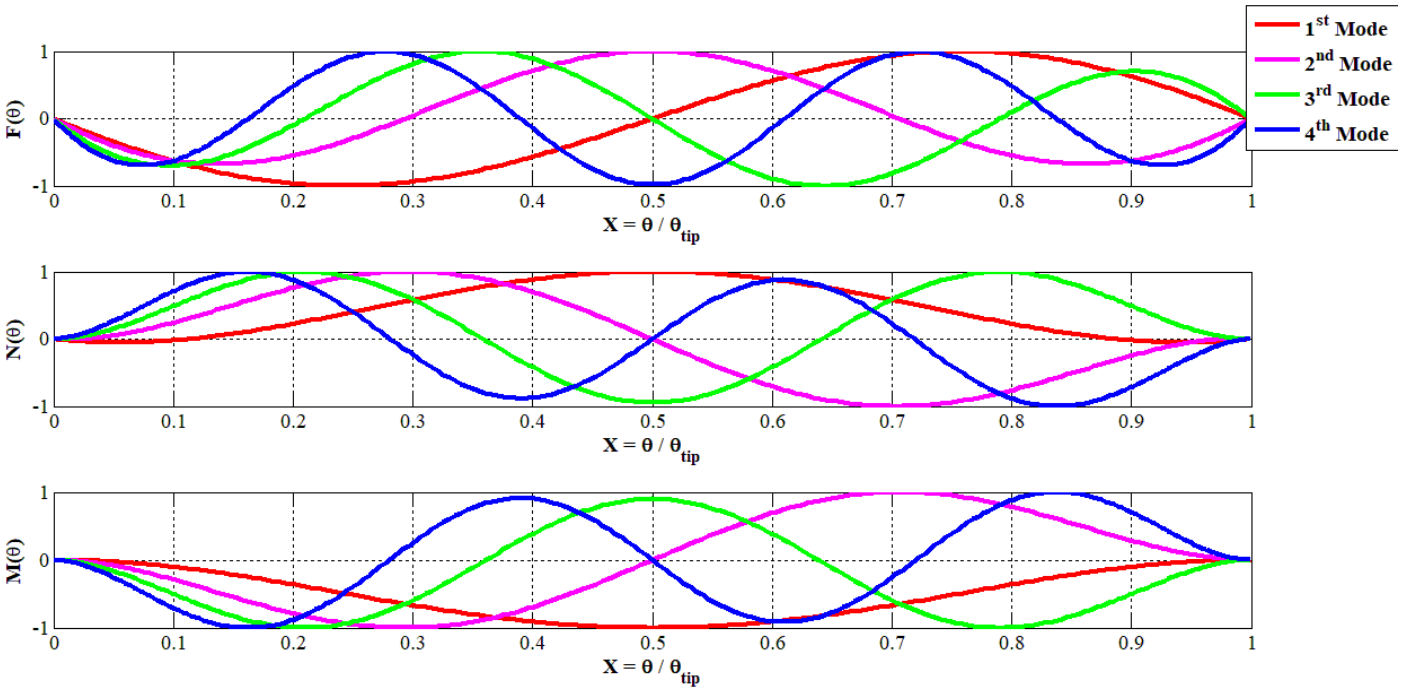

Bi-directional gradation ($\lambda_\theta = 1$)

Clamped-Clamped

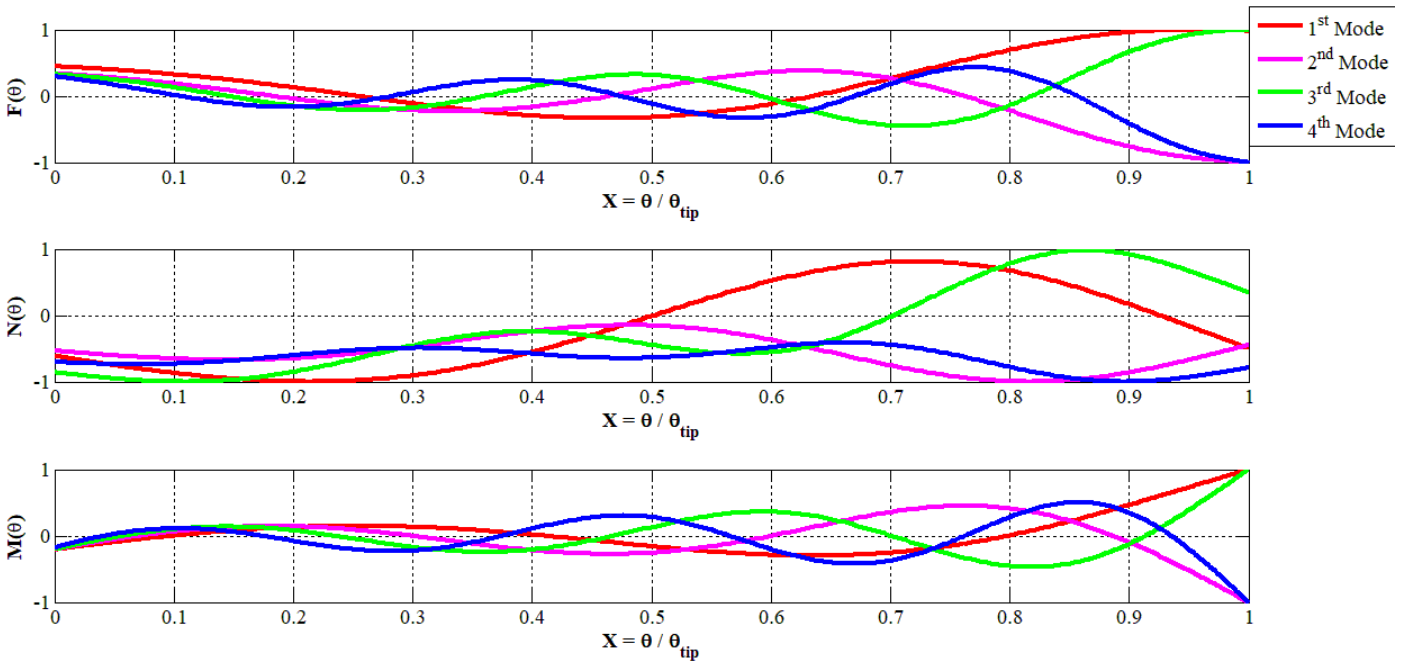

Hinged-Hinged

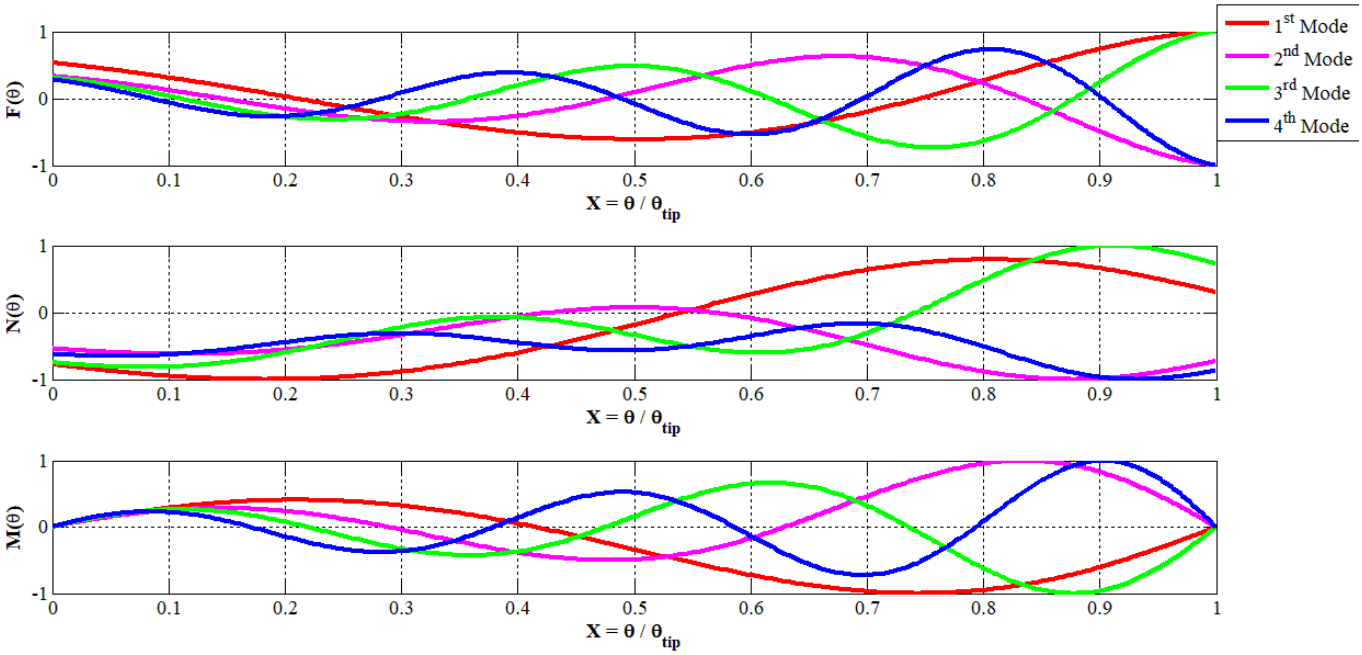

Free-Free

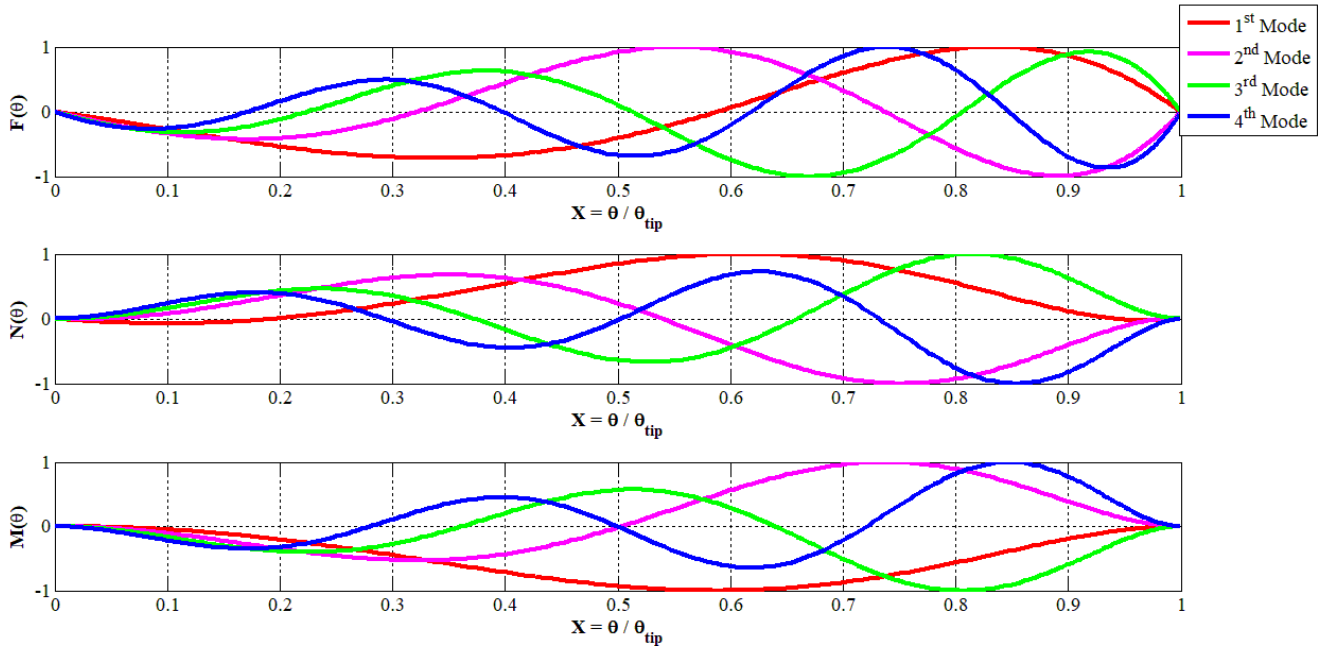

Figure 10 Normalized stress resultants for the first four mode shapes of a semi-circular FGM beam $(\theta_{tip} = \pi\, rad)$

4. Conclusions

We have studied free vibrations of a bi-directionally graded material circular beam by using a higher order shear deformable beam theory that has logarithmic variation in the radial direction of the tangential displacement. The beam theory exactly satisfies null tangential tractions on the top and the bottom surface, provides a quadratic through-the-thickness variation of the transverse shear strain, and does not need a shear correction factor. For clamped-clamped, hinged-hinged and free-free beams, we have used a generalized differential quadrature method to compute frequencies and mode shapes. Salient findings include that the spatial variation of material properties (mass density, shear modulus and Young's modulus) does not affect both the mode shapes and the angular width of the beam for which the first two modes of free vibrations have very close frequencies. This value is called the mode-transition width since shapes of modes one and two are interchanged for the beam angular width exceeding this value. For a clamped-clamped bi-directionally graded half-circular beam, the lowest frequency monotonically increases with an increase in the values of the two gradation indices in the postulated expressions for the material gradation. For beams of other angular widths and edge conditions, one can find the gradation indices to optimize the fundamental frequency.

Acknowledgements

RCB's work was partially funded by the Office of Naval Research (ONR) grant N00014-18-1-2548 to Virginia Polytechnic Institute and State University with Dr. Y. D. S. Rajapakse as the Program Manager.

BIBLIOGRAPHY

1. Huang, T.C., *The Effect of Rotatory Inertia and of Shear Deformation on the Frequency and Normal Mode Equations of Uniform Beams With Simple End Conditions.* Journal of Applied Mechanics, 1961. **28**(4): p. 579-584.
2. Bhimaraddi, A. and K. Chandrashekhara, *Observations on Higher‐Order Beam Theory.* Journal of Aerospace Engineering, 1993. **6**(4): p. 408-413.
3. Muhammad, A.K., M.H. Baluch, and A.K. Azad, *Generalized Theory for Bending of Thick Plates*, in *Studies in Applied Mechanics*, G.Z. Voyiadjis and D. Karamanlidis, Editors. 1990, Elsevier. p. 45-61.
4. Carrera, E., M. Filippi, and E. Zappino, *Laminated beam analysis by polynomial, trigonometric, exponential and zig-zag theories.* European Journal of Mechanics - A/Solids, 2013. **41**: p. 58-69.
5. Chandrashekhara, K. and K.M. Bangera, *Free vibration of composite beams using a refined shear flexible beam element.* Computers & Structures, 1992. **43**(4): p. 719-727.
6. Khdeir, A.A. and J.N. Reddy, *Free vibration of cross-ply laminated beams with arbitrary boundary conditions.* International Journal of Engineering Science, 1994. **32**(12): p. 1971-1980.
7. Koizumi, M., *FGM activities in Japan.* Composites Part B: Engineering, 1997. **28**(1): p. 1-4.
8. Sobczak, J.J. and L. Drenchev, *Metallic Functionally Graded Materials: A Specific Class of Advanced Composites.* Journal of Materials Science & Technology, 2013. **29**(4): p. 297-316.
9. Kadoli, R., K. Akhtar, and N. Ganesan, *Static analysis of functionally graded beams using higher order shear deformation theory.* Applied Mathematical Modelling, 2008. **32**(12): p. 2509-2525.
10. Li, X.F., *A unified approach for analyzing static and dynamic behaviors of functionally graded Timoshenko and Euler–Bernoulli beams.* Journal of Sound and Vibration, 2008. **318**(4): p. 1210-1229.
11. Şimşek, M., *Vibration analysis of a functionally graded beam under a moving mass by using different beam theories.* Composite Structures, 2010. **92**(4): p. 904-917.
12. Menaa, R., A. Tounsi, F. Mouaici, I. Mechab, M. Zidi, and E.A.A. Bedia, *Analytical Solutions for Static Shear Correction Factor of Functionally Graded Rectangular Beams.* Mechanics of Advanced Materials and Structures, 2012. **19**(8): p. 641-652.

13. Li, S.-R., D.-F. Cao, and Z.-Q. Wan, *Bending solutions of FGM Timoshenko beams from those of the homogenous Euler–Bernoulli beams.* Applied Mathematical Modelling, 2013. **37**(10): p. 7077-7085.

14. Jing, L.-l., P.-j. Ming, W.-p. Zhang, L.-r. Fu, and Y.-p. Cao, *Static and free vibration analysis of functionally graded beams by combination Timoshenko theory and finite volume method.* Composite Structures, 2016. **138**: p. 192-213.

15. Lü, C.F., W.Q. Chen, R.Q. Xu, and C.W. Lim, *Semi-analytical elasticity solutions for bi-directional functionally graded beams.* International Journal of Solids and Structures, 2008. **45**(1): p. 258-275.

16. Qian, L.F. and R.C. Batra, *Design of bidirectional functionally graded plate for optimal natural frequencies.* Journal of Sound and Vibration, 2005. **280**(1): p. 415-424.

17. Goupee, A.J. and S.S. Vel, *Optimization of natural frequencies of bidirectional functionally graded beams.* Structural and Multidisciplinary Optimization, 2006. **32**(6): p. 473-484.

18. Şimşek, M., *Bi-directional functionally graded materials (BDFGMs) for free and forced vibration of Timoshenko beams with various boundary conditions.* Composite Structures, 2015. **133**: p. 968-978.

19. Karamanlı, A., *Free vibration analysis of two directional functionally graded beams using a third order shear deformation theory.* Composite Structures, 2018. **189**: p. 127-136.

20. Rastgo, A., H. Shafie, and A. Allahverdizadeh, *Instability of Curved Beams Made of Functionally Graded Material Under Thermal Loading.* International Journal of Mechanics and Materials in Design, 2005. 2(1): p. 117-128.

21. Eroglu, U., *In-plane free vibrations of circular beams made of functionally graded material in thermal environment: Beam theory approach.* Composite Structures, 2015. 122: p. 217-228.

22. Pydah, A. and A. Sabale, *Static analysis of bi-directional functionally graded curved beams.* Composite Structures, 2017. 160: p. 867-876.

23. Pydah, A. and R.C. Batra, *Shear deformation theory using logarithmic function for thick circular beams and analytical solution for bi-directional functionally graded circular beams.* Composite Structures, 2017. **172**: p. 45-60.

24. Carrera, E., G. Giunta, and M. Petrolo, *Beam structures: classical and advanced theories*. 2011: John Wiley & Sons.

25. Tüfekçi, E. and A. Arpaci, *EXACT SOLUTION OF IN-PLANE VIBRATIONS OF CIRCULAR ARCHES WITH ACCOUNT TAKEN OF AXIAL EXTENSION, TRANSVERSE SHEAR AND ROTATORY INERTIA EFFECTS.* Journal of Sound and Vibration, 1998. **209**(5): p. 845-856.

26. Du, H., M. Lim, and R. Lin, *Application of generalized differential quadrature method to structural problems.* International Journal for Numerical Methods in Engineering, 1994. **37**(11): p. 1881-1896.

27. Filipich, C.P. and M.T. Piovan, *The dynamics of thick curved beams constructed with functionally graded materials.* Mechanics Research Communications, 2010. **37**(6): p. 565-570.

28. Tarnopolskaya, T., F.R. De Hoog, and N.H. Fletcher, *LOW-FREQUENCY MODE TRANSITION IN THE FREE IN-PLANE VIBRATION OF CURVED BEAMS.* Journal of Sound and Vibration, 1999. **228**(1): p. 69-90.

29. S. S. Vel and R. C. Batra, The Generalized Plane Strain Deformations of Thick Anisotropic Composite Laminated Plates, *Int. J. Solids Structures*, **37**, 715-733, 2000

30. Shafiee, H., M.H. Naei, and M.R. Eslami, *In-plane and out-of-plane buckling of arches made of FGM.* International Journal of Mechanical Sciences, 2006. **48**(8): p. 907-915.

31. R. C. Batra and G. M. Zhang, SSPH Basis Functions for Meshless Methods, and Comparison of Solutions with Strong and Weak Formulations, *Computational Mechanics*, **41**, 527-545, 2008.

32. G. M. Zhang and R. C. Batra, Symmetric Smoothed Particle Hydrodynamics (SSPH) Method and its Application to Elastic Problems, *Computational Mechanics*, **43**, 321-340, 2009.

33. R. C. Batra, Saint-Venant's Principle for a Helical Spring, *J. Appl. Mech*., **45**, 297-301, 1978.

Appendix

The MATLAB code for calculation of frequency parameters of a bi-directional FG semi-circular beam with clamped-clamped boundary conditions:

```
clear all;close all; clc;

% Determining the Domain & Meshing
n   = 25  ; % Number of Points on the beam
R   = 0.5;  % Beam's Radius
h   = 0.05   ; %Beam's Thickness
Rin = R-h/2;
Rout= R+h/2;

w   = 00.01:0.01:100 ; % The range of Natural Frequency
%U0 =( 4*(r^2-R0^2-2*R0*r*log(r/R0))/h^2 );
Z1  = zeros(n,1);       %Matrix Determinant
l   = pi;               %opening Angle

%% Determininig The X Matrix
[x,XX] = myPz(n,l);     %Coordinates of the points on the beam

% Creating C_ij
c   = myDQM(n,l);       % GDQ CoefficientsS

g1  = eye(n);           %Gradation Of material Along the beam
g2  = c;

for i=1:n
    for j=1:n

    g1(i,j) = g1(i,j)*exp(   -0.25* x(i));
    g2(i,j) = g2(i,j) * exp( -0.25* x(i));
    end
end


rho_out     = 3200;     %Mass Density
rho_in      = 7800;

E_out       = 390*10^9; %Young's Modulus
E_in        = 214*10^9;

G_out       = 137*10^9;
G_in        = 82.2*10^9;


% Radial Gradation of Material
```

```
% rho = (1 + (rho_in/rho_out - 1) * (1/2 - (r - R) / h))   ;
% E   = (1 + (E_in/E_out - 1) * (1/2 - (r - R) / h))   ;
% G   = (1 + (E_in/E_out - 1) * (1/2 - (r - R) / h))/(2*(1+0.3) ;



%% Calculution of Constant Coefficients

AA1  =   integral(@(r) (1 + (rho_in/rho_out - 1) .* (1/2 - (r - R) / h))...
    .*r                                              ,R-h/2,R+h/2);
AA2  =   integral(@(r) (1 + (rho_in/rho_out - 1) .* (1/2 - (r - R) / h))...
    .*r.^2                                           ,R-h/2,R+h/2);
AA3  =   integral(@(r) (1 + (rho_in/rho_out - 1) * (1/2 - (r - R) / h))...
    .*r.^3                                           ,R-h/2,R+h/2);

K0  =   integral(@(r) (1 + (rho_in/rho_out - 1) * (1/2 - (r - R) / h))...
    .*         ( 4*(r.^2-R^2-2*R*r.*log(r./R))/h^2 )           ,R-h/2,R+h/2);
K1  =   integral(@(r) (1 + (rho_in/rho_out - 1) * (1/2 - (r - R) / h))...
    .*r.*      ( 4*(r.^2-R^2-2*R*r.*log(r./R))/h^2 )           ,R-h/2,R+h/2);
K2  =   integral(@(r) (1 + (rho_in/rho_out - 1) * (1/2 - (r - R) / h))...
    .*r.^2.*   ( 4*(r.^2-R^2-2*R*r.*log(r./R))/h^2 )           ,R-h/2,R+h/2);
K3  =   integral(@(r) (1 + (rho_in/rho_out - 1) * (1/2 - (r - R) / h))...
    .*r.^3.*   ( 4.*(r.^2-R.^2-2*R*r.*log(r./R))/h.^2 )        ,R-h/2,R+h/2);

I0  =   integral(@(r) (1 + (rho_in/rho_out - 1) * (1/2 - (r - R) / h))...
    .*         (( 4*(r.^2-R^2-2*R*r.*log(r./R))/h^2 ).^2)      ,R-h/2,R+h/2);
I1  =   integral(@(r) (1 + (rho_in/rho_out - 1) * (1/2 - (r - R) / h))...
    .*r.*      (( 4*(r.^2-R^2-2*R*r.*log(r./R))/h^2 ).^2)      ,R-h/2,R+h/2);
I2  =   integral(@(r) (1 + (rho_in/rho_out - 1) * (1/2 - (r - R) / h))...
    .*r.^2.*   (( 4*(r.^2-R^2-2*R*r.*log(r./R))./h^2 ).^2)    ,R-h/2,R+h/2);


E0  =   integral(@(r) (1 + (E_in/E_out - 1) * (1/2 - (r - R) / h))...
    ./r                                              ,R-h/2,R+h/2);
E1  =   integral(@(r) (1 + (E_in/E_out - 1) * (1/2 - (r - R) / h))...
    .*r.^0                                           ,R-h/2,R+h/2);
E2  =   integral(@(r) (1 + (E_in/E_out - 1) * (1/2 - (r - R) / h))...
    .*r                                              ,R-h/2,R+h/2);


EE0  =   integral(@(r) (1 + (E_in/E_out - 1) * (1/2 - (r - R) / h))...
    ./r.*         ( 4*(r.^2-R^2-2*R*r.*log(r./R))/h^2 )           ,R-h/2,R+h/2);
EE1  =   integral(@(r) (1 + (E_in/E_out - 1) * (1/2 - (r - R) / h))...
    .*          ( 4*(r.^2-R^2-2*R*r.*log(r./R))/h^2 )           ,R-h/2,R+h/2);
EE2  =   integral(@(r) (1 + (E_in/E_out - 1) * (1/2 - (r - R) / h))...
    .*r.*        ( 4*(r.^2-R^2-2*R*r.*log(r./R))/h^2 )           ,R-h/2,R+h/2);


EEE0  =   integral(@(r) (1 + (E_in/E_out - 1) * (1/2 - (r - R) / h))...
    ./r.*         ( 4*(r.^2-R^2-2*R*r.*log(r./R))/h^2 ).^2          ,R-
h/2,R+h/2);
EEE1  =   integral(@(r) (1 + (E_in/E_out - 1) * (1/2 - (r - R) / h))...
    .*          ( 4*(r.^2-R^2-2*R*r.*log(r./R))/h^2 ).^2          ,R-h/2,R+h/2);
```

```
G0  =   integral(@(r) (  G_out + ( G_in - G_out ) * ( 0.5 - ( r-R )/h ) )/G_out./r
,R-h/2,R+h/2);
G1  =   integral(@(r) (  G_out + ( G_in - G_out ) * ( 0.5 - ( r-R )/h )
)/G_out.*r.^0                                          ,R-h/2,R+h/2);
G2  =   integral(@(r) (  G_out + ( G_in - G_out ) * ( 0.5 - ( r-R )/h ) )/G_out.*r
,R-h/2,R+h/2);
G3  =   integral(@(r) (  G_out + ( G_in - G_out ) * ( 0.5 - ( r-R )/h )
)/G_out.*r.^2                                            ,R-h/2,R+h/2);
G4  =   integral(@(r) (  G_out + ( G_in - G_out ) * ( 0.5 - ( r-R )/h )
)/G_out.*r.^3                                            ,R-h/2,R+h/2);
```

```
for i=1:length(w)
%% Construction of the Coefficent Matrix

        A1 = zeros(7*n);

        A1(1:n,1:n) = 1/l^4 *  1/12 * (h/R)^3 * w(i)^2 * AA1/(R*h) * g1;
%Ur
        A1(1:n,4*n+1:5*n) = c;
%F
        A1(1:n,5*n+1:6*n) = -eye(n,n);
%N
```

```
        A1(n+1:2*n,n+1:2*n)   = 1/l^4 * 1/12 * (h/R)^3 * (-K1/(R*h) ) * w(i)^2 *
g1;   %U1
        A1(n+1:2*n,2*n+1:3*n) = 1/l^4 * 1/12 * (h/R)^3 * (AA1/(R*h) +  K1/(R*h)) *
w(i)^2 * g1;%Utheta
        A1(n+1:2*n,3*n+1:4*n) = 1/l^4 *  1/12 * (h/R)^3  * (AA2/(R) - AA1 - K1
)/(R*h) * w(i)^2 * g1;%phi
        A1(n+1:2*n,4*n+1:5*n) = eye(n,n);
%F
        A1(n+1:2*n,5*n+1:6*n) = c;
%N
```

```
        A1(2*n+1:3*n,n+1:2*n)   = 1/l^4 *  (-1)/12 * (h/R)^3 * 1/(R*h) * (K2/R -
K1 ) * w(i)^2 * g1; %U1
        A1(2*n+1:3*n,2*n+1:3*n) = 1/l^4 *  1/12 * (h/R)^3 * 1/(R*h) * ( AA2/R -
AA1 - K1 + K2/R ) * w(i)^2 * g1; %Utheta
        A1(2*n+1:3*n,3*n+1:4*n) = 1/l^4 *  1/12 * (h/R)^3 * 1/(R*h) * (AA3/(R^2) +
AA1 -2*AA2/R - K2/R + K1) * w(i)^2 * g1; %phi
        A1(2*n+1:3*n,4*n+1:5*n) = -eye(n,n);%F
        A1(2*n+1:3*n,6*n+1:7*n) = c;%M
```

```
        A1(3*n+1:4*n,1:n) = c;%Ur
        A1(3*n+1:4*n,n+1:2*n) = -eye(n,n);%U1


        A1(4*n+1:5*n,1:n) =  (G0* (1 - 4*(R/h)^2) - 4*G2/h^2 + 8*G1*R/h^2) * g2;
        A1(4*n+1:5*n,2*n+1:3*n) =  - (G0* (1 - 4*(R/h)^2) - 4*G2/h^2 + 8*G1*R/h^2)
* g1;
        A1(4*n+1:5*n,3*n+1:4*n) = (G0* (1 - 4*(R/h)^2) - 4*G2/h^2 + 8*G1*R/h^2) *
g1;
        A1(4*n+1:5*n,4*n+1:5*n) = -eye(n,n);                % F Definition


        A1(5*n+1:6*n,1:n) = E0*g1;
        A1(5*n+1:6*n,n+1:2*n) = -EE0*g2;
        A1(5*n+1:6*n,2*n+1:3*n) = (E0 + EE0) * g2;
        A1(5*n+1:6*n,3*n+1:4*n) = (E1/R - E0 - EE0) * g2;
        A1(5*n+1:6*n,5*n+1:6*n) = -eye(n,n);% N Definition


        A1(6*n+1:7*n,1:n) = (E1/R - E0)*g1;
        A1(6*n+1:7*n,n+1:2*n) = (EE0 - EE1/R)*g2;
        A1(6*n+1:7*n,2*n+1:3*n) = (E1/R + EE1/R - E0 - EE0)*g2;
        A1(6*n+1:7*n,3*n+1:4*n) = (E2/R^2 - 2*E1/R - EE1/R + EE0 + E0)*g2;
        A1(6*n+1:7*n,6*n+1:7*n) = -eye(n,n); %M Definition


 %% Applying the Boundry Conditions

        A2 = A1;

        A2(4*n,:)   = [];   % phi(n)
        A2(3*n+1,:) = [];   % phi(1)
        A2(3*n,:)   = [];   % Utheta(n)
        A2(2*n+1,:) = [];   % Utheta(1)
        A2(n,:)     = [];   % Ur(n)
        A2(1,:)     = [];   % Ur(1)



        A2(:,4*n)   = [];
        A2(:,3*n+1) = [];
        A2(:,3*n)   = [];
        A2(:,2*n+1) = [];
        A2(:,n)     = [];
        A2(:,1)     = [];


        Z1(i) = det(A2);
end

plot(w,Z1)
```

The MATLAB code for plotting normalized the mode shapes, displacement components and stress resultants of a bi-directional FG semi-circular beam with clamped-clamped boundary conditions:

```
clear all;close all; clc;

color1=['r' 'm' 'g' 'b'];

% Determining the Domain & Meshing
n   = 401  ;
R   = 0.5  ;
h   = 0.05   ;
Rin = R-h/2;
Rout= R+h/2;

w   = [28.29 60.87 112.45 162.9] ;
%U0 =( 4*(r^2-R0^2-2*R0*r*log(r/R0))/h^2 );
Z1  = zeros(n,1);
l   = pi;

%% Determininig The X Matrix
[x,XX] = myPz(n,l);

% Creating C_ij


c   = myDQM(n,l);

g1  = eye(n);
g2  = c;

for i=1:n
    for j=1:n

    g1(i,j) = g1(i,j)*exp(-0.25 * x(i));
    g2(i,j) = g2(i,j) * exp(-0.25 * x(i));
    end
end



rho = 1;
E   = 1;
G   = E/(2*(1+0.3)) ;

rho_out     = 3200;
rho_in      = 7800;

E_out       = 390*10^9;
E_in        = 214*10^9;
```

```
G_out       = 137*10^9;
G_in        = 82.2*10^9;

% rho = (1 + (rho_in/rho_out - 1) * (1/2 - (r - R) / h))   ;
% E   = (1 + (E_in/E_out - 1) * (1/2 - (r - R) / h))   ;
% G   = (1 + (E_in/E_out - 1) * (1/2 - (r - R) / h))/(2*(1+0.3) ;



% AA0  =   integral(@(r) rho./r                                          ,R-
h/2,R+h/2);
AA1  =   integral(@(r) (1 + (rho_in/rho_out - 1) .* (1/2 - (r - R) / h))...
    .*r                                          ,R-h/2,R+h/2);
AA2  =   integral(@(r) (1 + (rho_in/rho_out - 1) .* (1/2 - (r - R) / h))...
    .*r.^2                                       ,R-h/2,R+h/2);
AA3  =   integral(@(r) (1 + (rho_in/rho_out - 1) * (1/2 - (r - R) / h))...
    .*r.^3                                       ,R-h/2,R+h/2);

K0  =   integral(@(r) (1 + (rho_in/rho_out - 1) * (1/2 - (r - R) / h))...
    .*         ( 4*(r.^2-R^2-2*R*r.*log(r./R))/h^2 )           ,R-h/2,R+h/2);
K1  =   integral(@(r) (1 + (rho_in/rho_out - 1) * (1/2 - (r - R) / h))...
    .*r.*      ( 4*(r.^2-R^2-2*R*r.*log(r./R))/h^2 )           ,R-h/2,R+h/2);
K2  =   integral(@(r) (1 + (rho_in/rho_out - 1) * (1/2 - (r - R) / h))...
    .*r.^2.*   ( 4*(r.^2-R^2-2*R*r.*log(r./R))/h^2 )           ,R-h/2,R+h/2);
K3  =   integral(@(r) (1 + (rho_in/rho_out - 1) * (1/2 - (r - R) / h))...
    .*r.^3.*   ( 4.*(r.^2-R.^2-2*R*r.*log(r./R))/h.^2 )        ,R-h/2,R+h/2);

I0  =   integral(@(r) (1 + (rho_in/rho_out - 1) * (1/2 - (r - R) / h))...
    .*         (( 4*(r.^2-R^2-2*R*r.*log(r./R))/h^2 ).^2)      ,R-h/2,R+h/2);
I1  =   integral(@(r) (1 + (rho_in/rho_out - 1) * (1/2 - (r - R) / h))...
    .*r.*      (( 4*(r.^2-R^2-2*R*r.*log(r./R))/h^2 ).^2)      ,R-h/2,R+h/2);
I2  =   integral(@(r) (1 + (rho_in/rho_out - 1) * (1/2 - (r - R) / h))...
    .*r.^2.*   (( 4*(r.^2-R^2-2*R*r.*log(r./R))./h^2 ).^2)    ,R-h/2,R+h/2);


E0  =   integral(@(r) (1 + (E_in/E_out - 1) * (1/2 - (r - R) / h))...
    ./r                                          ,R-h/2,R+h/2);
E1  =   integral(@(r) (1 + (E_in/E_out - 1) * (1/2 - (r - R) / h))...
    .*r.^0                                       ,R-h/2,R+h/2);
E2  =   integral(@(r) (1 + (E_in/E_out - 1) * (1/2 - (r - R) / h))...
    .*r                                          ,R-h/2,R+h/2);


EE0  =   integral(@(r) (1 + (E_in/E_out - 1) * (1/2 - (r - R) / h))...
    ./r.*         ( 4*(r.^2-R^2-2*R*r.*log(r./R))/h^2 )           ,R-h/2,R+h/2);
EE1  =   integral(@(r) (1 + (E_in/E_out - 1) * (1/2 - (r - R) / h))...
    .*          ( 4*(r.^2-R^2-2*R*r.*log(r./R))/h^2 )           ,R-h/2,R+h/2);
EE2  =   integral(@(r) (1 + (E_in/E_out - 1) * (1/2 - (r - R) / h))...
    .*r.*        ( 4*(r.^2-R^2-2*R*r.*log(r./R))/h^2 )           ,R-h/2,R+h/2);


EEE0  =   integral(@(r) (1 + (E_in/E_out - 1) * (1/2 - (r - R) / h))...
    ./r.*         ( 4*(r.^2-R^2-2*R*r.*log(r./R))/h^2 ).^2          ,R-
h/2,R+h/2);
```

```
EEE1  =   integral(@(r) (1 + (E_in/E_out - 1) * (1/2 - (r - R) / h))...
    .*           ( 4*(r.^2-R^2-2*R*r.*log(r./R))/h^2 ).^2           ,R-h/2,R+h/2);


G0  =   integral(@(r) (  G_out + ( G_in - G_out ) * ( 0.5 - ( r-R )/h ) )/G_out./r
,R-h/2,R+h/2);
G1  =   integral(@(r) (  G_out + ( G_in - G_out ) * ( 0.5 - ( r-R )/h )
)/G_out.*r.^0                                          ,R-h/2,R+h/2);
G2  =   integral(@(r) (  G_out + ( G_in - G_out ) * ( 0.5 - ( r-R )/h ) )/G_out.*r
,R-h/2,R+h/2);
G3  =   integral(@(r) (  G_out + ( G_in - G_out ) * ( 0.5 - ( r-R )/h )
)/G_out.*r.^2                                            ,R-h/2,R+h/2);
G4  =   integral(@(r) (  G_out + ( G_in - G_out ) * ( 0.5 - ( r-R )/h )
)/G_out.*r.^3                                            ,R-h/2,R+h/2);

  xx  = x;
  xx(n)=[];
  xxx = xx;
  xxx(4)=[];
  xxx(1)=[];
  xx(1)=[];


  xcoordinate = x - l/2 ;
  xxcoordinate = xx - l/2 ;
  xxxcoordinate = xxx - l/2 ;

for i=1:length(w)

% Coefficent Matrix %%%%%%%%%%%%%%%%%%%%%%%%%%%%%%%%%%%%%%%%%%%%

        A1 = zeros(7*n);

        A1(1:n,1:n) = 1/l^4 *  1/12 * (h/R)^3 * w(i)^2 * AA1/(R*h) * g1;
%Ur
        A1(1:n,4*n+1:5*n) = c;
%F
        A1(1:n,5*n+1:6*n) = -eye(n,n);
%N




        A1(n+1:2*n,n+1:2*n)   = 1/l^4 * 1/12 * (h/R)^3 * (-K1/(R*h) ) * w(i)^2 *
g1;   %U1
        A1(n+1:2*n,2*n+1:3*n) = 1/l^4 * 1/12 * (h/R)^3 * (AA1/(R*h) +  K1/(R*h)) *
w(i)^2 * g1;%Utheta
        A1(n+1:2*n,3*n+1:4*n) = 1/l^4 *  1/12 * (h/R)^3  * (AA2/(R) - AA1 - K1
)/(R*h) * w(i)^2 * g1;%phi
        A1(n+1:2*n,4*n+1:5*n) = eye(n,n);
%F
        A1(n+1:2*n,5*n+1:6*n) = c;
%N
```

```
        A1(2*n+1:3*n,n+1:2*n)   = 1/l^4 *  (-1)/12 * (h/R)^3 * 1/(R*h) * (K2/R -
K1 ) * w(i)^2 * g1;
        A1(2*n+1:3*n,2*n+1:3*n) = 1/l^4 *  1/12 * (h/R)^3 * 1/(R*h) * ( AA2/R -
AA1 - K1 + K2/R ) * w(i)^2 * g1;
        A1(2*n+1:3*n,3*n+1:4*n) = 1/l^4 *  1/12 * (h/R)^3 * 1/(R*h) * (AA3/(R^2) +
AA1 -2*AA2/R - K2/R + K1) * w(i)^2 * g1;
        A1(2*n+1:3*n,4*n+1:5*n) = -eye(n,n);
        A1(2*n+1:3*n,6*n+1:7*n) = c;



        A1(3*n+1:4*n,1:n) = c;
        A1(3*n+1:4*n,n+1:2*n) = -eye(n,n);


        A1(4*n+1:5*n,1:n) =  (G0* (1 - 4*(R/h)^2) - 4*G2/h^2 + 8*G1*R/h^2) * g2;
        A1(4*n+1:5*n,2*n+1:3*n) =  - (G0* (1 - 4*(R/h)^2) - 4*G2/h^2 + 8*G1*R/h^2)
* g1;
        A1(4*n+1:5*n,3*n+1:4*n) = (G0* (1 - 4*(R/h)^2) - 4*G2/h^2 + 8*G1*R/h^2) *
g1;
        A1(4*n+1:5*n,4*n+1:5*n) = -eye(n,n);                % F Definition


        A1(5*n+1:6*n,1:n) = E0*g1;
        A1(5*n+1:6*n,n+1:2*n) = -EE0*g2;
        A1(5*n+1:6*n,2*n+1:3*n) = (E0 + EE0) * g2;
        A1(5*n+1:6*n,3*n+1:4*n) = (E1/R - E0 - EE0) * g2;
        A1(5*n+1:6*n,5*n+1:6*n) = -eye(n,n);


        A1(6*n+1:7*n,1:n) = (E1/R - E0)*g1;
        A1(6*n+1:7*n,n+1:2*n) = (EE0 - EE1/R)*g2;
        A1(6*n+1:7*n,2*n+1:3*n) = (E1/R + EE1/R - E0 - EE0)*g2;
        A1(6*n+1:7*n,3*n+1:4*n) = (E2/R^2 - 2*E1/R - EE1/R + EE0 + E0)*g2;
        A1(6*n+1:7*n,6*n+1:7*n) = -eye(n,n);




 % Boundry Conditions %%%%%%%%%%%%%%%%%%%%%%%%%%%%%%%%%%%%%%%

        A2 = A1;

        A2(4*n,:)   = [];
        A2(3*n+1,:) = [];
        A2(3*n,:)   = [];
        A2(2*n+1,:) = [];
        A2(n,:)     = [];
        A2(5,:)= [];
        A2(1,:)     = [];
```

```
        A2(:,4*n)   = [];
        A2(:,3*n+1) = [];
        A2(:,3*n)   = [];
        A2(:,2*n+1) = [];
        A2(:,n)     = [];
        A2(:,5)     = [];
        A2(:,1)     = [];



        B1 = -A1(:,5);
        B1(4*n,:)   = [];
        B1(3*n+1,:) = [];
        B1(3*n,:)   = [];
        B1(2*n+1,:) = [];
        B1(n,:)     = [];
        B1(5,:)     = [];
        B1(1,:)     = [];




       Sol(:,i) = A2\B1 ;

ur = Sol(1:n-3,i) / max( [max(abs(Sol(1:n-3,i))) max(abs(Sol(2*n-2:3*n-5,i)))]
)/10;
ut = Sol(2*n-2:3*n-5,i) / max( [max(abs(Sol(1:n-3,i))) max(abs(Sol(2*n-2:3*n-
5,i)))] )/10;

ut(5,:)=[];

figure(1)
subplot(2,2,1)
plot(xxx/l,Sol(1:n-3,i)/max(abs(Sol(1:n-3,i))),'LineWidth',2,'linestyle','-
','color',color1(i))

ylabel('u_r^0','FontSize',14)
xlabel('X = \theta / \theta_0','FontSize',14)
% title('FG beam with exponential radial gradation of properties
CC','FontSize',14)
title('(a)','FontSize',14)
legend('1^s^t Mode' , '2^n^d Mode' , '3^r^d Mode' , '4^t^h Mode');
grid on
hold on

% figure(2)
subplot(2,2,2)
plot(x/l,Sol(n-2:2*n-3,i)/max(abs(Sol(n-2:2*n-3,i))),'LineWidth',2,'linestyle','-
','color',color1(i))

ylabel('u_1','FontSize',14)
xlabel('X = \theta / \theta_0','FontSize',14)
```

```
% title('FG beam with exponential radial gradation of properties
CC','FontSize',14)
title('(b)','FontSize',14)
legend('1^s^t Mode' , '2^n^d Mode' , '3^r^d Mode' , '4^t^h Mode');
grid on
hold on

subplot(2,2,3)
plot(xx/l,Sol(2*n-2:3*n-5,i)/max(abs(Sol(2*n-2:3*n-
5,i))),'LineWidth',2,'linestyle','-','color',color1(i))

ylabel('u_\theta','FontSize',14)
xlabel('X = \theta / \theta_0','FontSize',14)
% title('FG beam with exponential radial gradation of properties
CC','FontSize',14)
title('(c)','FontSize',14)
legend('1^s^t Mode' , '2^n^d Mode' , '3^r^d Mode' , '4^t^h Mode');
grid on
hold on


subplot(2,2,4)
plot(xx/l,Sol(3*n-4:4*n-7,i)/max(abs(Sol(3*n-4:4*n-
7,i))),'LineWidth',2,'linestyle','-','color',color1(i))

ylabel('\phi','FontSize',14)
xlabel('X = \theta / \theta_0','FontSize',14)
% title('FG beam with exponential radial gradation of properties
CC','FontSize',14)
title('(d)','FontSize',14)
legend('1^s^t Mode' , '2^n^d Mode' , '3^r^d Mode' , '4^t^h Mode');
grid on
hold on




figure(2)
subplot(3,1,1)
plot(x/l,Sol(4*n-6:5*n-7,i)/max(abs(Sol(4*n-6:5*n-
7,i))),'LineWidth',2,'linestyle','-','color',color1(i))

ylabel('F','FontSize',14)
xlabel('X = \theta / \theta_0','FontSize',14)
% title('FG beam with exponential radial gradation of properties
CC','FontSize',14)
title('(a)','FontSize',14)
legend('1^s^t Mode' , '2^n^d Mode' , '3^r^d Mode' , '4^t^h Mode');
grid on
hold on


subplot(3,1,2)
plot(x/l,Sol(5*n-6:6*n-7,i)/max(abs(Sol(5*n-6:6*n-
7,i))),'LineWidth',2,'linestyle','-','color',color1(i))
```

```
ylabel('N','FontSize',14)
xlabel('X = \theta / \theta_0','FontSize',14)
% title('FG beam with exponential radial gradation of properties
CC','FontSize',14)
title('(b)','FontSize',14)
legend('1^s^t Mode' , '2^n^d Mode' , '3^r^d Mode' , '4^t^h Mode');
grid on
hold on

subplot(3,1,3)
plot(x/l,Sol(6*n-6:7*n-7,i)/max(abs(Sol(6*n-6:7*n-
7,i))),'LineWidth',2,'linestyle','-','color',color1(i))

ylabel('M','FontSize',14)
xlabel('X = \theta / \theta_0','FontSize',14)
% title('FG beam with exponential radial gradation of properties
CC','FontSize',14)
title('(c)','FontSize',14)
legend('1^s^t Mode' , '2^n^d Mode' , '3^r^d Mode' , '4^t^h Mode');
grid on
hold on









figure(3)


plot(sin((xxxcoordinate)').*(R+ur) + cos((xxxcoordinate)').*ut ,
cos((xxxcoordinate)').*(R+ur) + sin((xxxcoordinate)').*ut
,'LineWidth',2,'linestyle','-','color',color1(i))


% title('FG beam with exponential radial gradation of properties
HH','FontSize',14)
title('(a)','FontSize',14)
% legend('1^s^t Mode' , '2^n^d Mode' , '3^r^d Mode' , '4^t^h Mode', 'Initial
Shape');

hold on

end


plot(sin((xxxcoordinate)').*(R) ,
cos((xxxcoordinate)').*(R),'LineWidth',3,'linestyle','-','color','k')
legend('1^s^t Mode' , '2^n^d Mode' , '3^r^d Mode' , '4^t^h Mode', 'Undeformed
Beam');
```

Definition of the Function myPz:

```
function [fun1,fun2] = myPz(N,L)

z   = zeros(1,N);
Pz  = ones(1,N);

% Defining xi_i
for i = 1:N
    z(i) = L*(0.5)*(  1 - cos( pi*(i-1)/(N-1) )  );
end

% Defining Product of (xi_i - zi_j)
for i = 1:N
    for v = 1:N
        if i ~= v
            Pz(i) = Pz(i) * (z(i)-z(v));
        end
    end
end

fun1 = z;
fun2 = Pz;
```

Definition of the Function myDQM:

```
function A = myDQM(N,L)

[z,Pz] = myPz(N,L);

%% Defining A^1_ij
A  = zeros(N,N);
for i = 1:N
    for j = 1:N
        if i ~= j
            A(i,j) = Pz(i) / (z(i)-z(j)) / Pz(j);
        end
    end
end
for i = 1:N
    for v = 1:N
        if i ~= v
            A(i,i) = A(i,i) - A(i,v);
        end
    end
end
```

*Functions myPz and myDQM must exist in the same folder as the MATLAB codes.